https://doi.org/10.5194/egusphere-2024-1768
Preprint. Discussion started: 1 July 2024

Characterization of biogenic volatile organic compounds and their oxidation products at a stressed pine forest close to a biogas power plant

Junwei Song[1,4*], Georgios I. Gkatzelis[2], Ralf Tillmann[2], Nicolas Brüggemann[3], Thomas Leisner[1] and Harald Saathoff[1,*]

[1] Institute of Meteorology and Climate Research, Karlsruhe Institute of Technology, Hermann-von-Helmholtz-Platz 1, 76344 Eggenstein-Leopoldshafen, Germany

[2] Institute of Energy and Climate Research, IEK-8: Troposphere, Forschungszentrum Jülich GmbH, 52425 Jülich, Germany

[3] Institute of Bio- and Geosciences, IBG-3: Agrosphere, Forschungszentrum Jülich GmbH, 52425 Jülich, Germany

[4] Université Claude Bernard Lyon 1, CNRS, IRCELYON, UMR 5256, F-69626, Villeurbanne, France

Correspondence: Junwei Song (junwei.song@ircelyon.univ-lyon1.fr) and Harald Saathoff (harald.saathoff@kit.edu)

https://doi.org/10.5194/egusphere-2024-1768
Preprint. Discussion started: 1 July 2024

Abstract

In this study, we present real-time measurements of organic aerosol (OA) and biogenic volatile organic compounds (BVOCs) at a pine forest stressed by bark beetles and previous droughts close to a biogas power plant (BPP) in western Germany during June 2020. A proton-transfer-reaction time-of-flight mass spectrometer coupled with a particle inlet (CHARON-PTR-ToF-MS) and a Vocus-PTR-ToF-MS were deployed to measure OA and BVOCs. During the entire measurement period, the average concentration of monoterpenes (2.5 ± 5.3 ppb) was higher than isoprene (0.58 ± 0.54 ppb) and sesquiterpenes (0.01 ± 0.01 ppb). The OA composition mainly consisted of semi-volatile organic compounds formed from monoterpene oxidation. Based on a wind direction analysis, BVOC data were categorized into two groups with main influence from the BPP (WD-BPP) and the forest (WD-forest), respectively. In the WD-BPP group, high concentrations of monoterpenes and sesquiterpenes were attributed to BPP emissions. In the WD-forest group, higher temperatures enhanced the biogenic emissions of isoprene, monoterpenes, and sesquiterpenes especially during daytime, exceeding their photochemical consumption. Positive matrix factorization analysis of VOCs revealed substantial contributions of gaseous organic acids from BVOC oxidation during daytime, while weakly oxidized monoterpene products dominated during nighttime. Moreover, increasing relative humidity promoted the gas-to-particle partitioning of gaseous weakly oxidized monoterpene products, leading to an increase of nighttime OA mass. This study highlights that the variations of BVOCs and their oxidation products are influenced by meteorology, local BPP emissions, and chemical transformation processes at this stressed forest.

1 Introduction

Volatile organic compounds (VOCs) play important roles in determining atmospheric chemical processes (Atkinson, 2000; Hallquist et al., 2009; Yáñez-Serrano et al., 2020; Shrivastava et al., 2017). Terrestrial ecosystems emit large amounts of biogenic VOCs (BVOCs, >1000 Tg yr^{-1}) to the global atmosphere, more than anthropogenic VOCs (AVOCs, ~200 Tg yr^{-1}) (Guenther et al., 2012; Sindelarova et al., 2014). BVOCs emitted by vegetation consist largely of reactive terpenoids e.g., isoprene (~70%), monoterpenes (~11%) and sesquiterpenes (~2.5%) (Sindelarova et al., 2014). The oxidation products of terpenoids can nucleate to form new particles or contribute to the growth of existing particles and secondary organic aerosol (SOA) formation, thus impacting air quality and climate (Hallquist et al., 2009; Shrivastava et al., 2017).

https://doi.org/10.5194/egusphere-2024-1768
Preprint. Discussion started: 1 July 2024

Over the last decade, several field studies have been conducted at different forests to investigate the characteristics of BVOCs including the emissions, temporal variations as well as their impacts on atmospheric reactivity and SOA formation (Hakola et al., 2012; Hellén et al., 2018; Li et al., 2020; Huang et al., 2021; Yáñez-Serrano et al., 2021; Vestenius et al., 2021; Mermet et al., 2021; Vermeuel et al., 2023). The diurnal pattern of isoprene concentrations in forests showed typically higher concentrations during daytime (Yáñez-Serrano et al., 2021; Yáñez-Serrano et al., 2015; Li et al., 2020; Hakola et al., 2012), since isoprene emissions increase with temperature and sunlight. The emissions and compositions of BVOCs from trees varies with abiotic and biotic stresses such as high temperature, drought and herbivore attack (Loreto and Schnitzler, 2010; Teskey et al., 2015; Jaakkola et al., 2023; Kari et al., 2019; Faiola and Taipale, 2020). It has been widely reported that these stresses can significantly alter the emissions of terpenoids (Ghimire et al., 2016; Jaakkola et al., 2023; Amin et al., 2012).

In addition to biogenic emissions, the temporal variations of BVOC concentrations especially of terpenoids are influenced by atmospheric oxidation processes. The diurnal variations of monoterpene concentrations generally showed lower values during daytime in the boreal forests, which were attributed to the rapid photochemical consumption and expanded boundary layer heights (Hellén et al., 2018; Hakola et al., 2012). Correspondingly, higher concentrations of monoterpene oxidation products are expected to be produced during daytime. For instance, Huang et al., (2021) found that some gaseous monoterpene oxidation products e.g., $C_7H_{10}O_4$ (3,6-oxoheptanoic acid) and $C_8H_{12}O_4$ (terpenylic acid) showed higher concentrations during daytime in a boreal forest. Li et at., (2020) reported similar diurnal variations of gaseous higher-oxidized monoterpene products (e.g., $C_8H_{12}O_{4\text{-}6}$, $C_9H_{14}O_{4\text{-}6}$, $C_{10}H_{14}O_{4\text{-}6}$ and $C_{10}H_{16}O_{4\text{-}6}$) in the Landes-forest in France. The variations of BVOC oxidation products are also influenced by gas-particle partitioning processes. Laboratory studies have shown that decreasing temperature and increasing relative humidity (RH) can lead to an increased particulate fraction of SOA products from BVOC oxidation (Surdu et al., 2023; Von Hessberg et al., 2009; Tillmann et al., 2010; Zhang et al., 2015; Luo et al., 2024). However, due to lack of online dual-phase measurements only few field studies have focused on the gas-particle partitioning of BVOC oxidation products in the real forest atmosphere (Mohr et al., 2017; Yatavelli et al., 2014; Isaacman-Vanwertz et al., 2016; Lee et al., 2018). Stress conditions like high temperature could not only increase BVOC emissions, but also result in variations of BVOC oxidation products and SOA formation. In the context of a warming climate and frequent insect outbreaks, it is necessary to investigate the variations of BVOC concentrations and their oxidation process for stressed forests (Faiola and Taipale, 2020).

https://doi.org/10.5194/egusphere-2024-1768
Preprint. Discussion started: 1 July 2024

The Eifel is low mountain range in western Germany that stretches across the federal states of North Rhine-Westphalia and Rhineland-Palatinate and covers an area of ~5300 km^2. Its forested areas are largely composed of Norway spruce and European beech trees, which are important contributors to BVOCs (Smiatek and Steinbrecher, 2006; Kleist et al., 2012). The Eifel Forest was suffering from severe droughts, heatwaves and severe bark beetle infestation in the years before our measurements (Weber et al., 2022; Montzka et al., 2021; Ghimire et al., 2016), and thus can be regarded as a stressed forest. In this study, a field measurement campaign was conducted at a site of the Eifel Forest in the vicinity of a biogas power plant (BPP). There are increasing numbers of BPPs distributed in European rural areas (Bakkaloglu et al., 2021; Scheftelowitz et al., 2018), which emit large amounts of CH_4 and VOCs periodically to the atmosphere around the BPPs (Salazar Gómez et al., 2016). In this paper, we present the real-time measurements of VOCs and aerosol particles measured by a proton-transfer-reaction time-of-flight mass spectrometer (PTR-ToF-MS) coupled with a particle inlet (CHARON, chemical analysis of aerosol online) and a Vocus-PTR-ToF-MS. The impacts of weather conditions, sources and chemical oxidation processes on the variations of BVOCs and their gaseous and particulate oxidation products were investigated to get a better understanding of BVOC emissions from stressed forests and their contributions to SOA as well as the potential impact of emissions from BPPs.

2 Methods

2.1 Sampling site

In this study, a three-week field campaign was conducted in the Eifel Forest (50.72° N, 6.40° E) during June 2020 as a part of the "Heat and Drought 2020" campaign of the Modular Observation Solutions of Earth Systems (MOSES) project of the Helmholtz Association of German Research Centers. As shown in Fig. 1a, the sampling site is located ~400 m southeast of a football field in the small village Kleinhau belonging to the municipality of Hürtgenwald, Germany (population about 9000) and ~250 m east of a BPP (BioEnergie Kleinhau GmbH). The biomass substrate used for the biogas production in this BPP consisted mainly of crop waste (e.g., corn stover). The forest extended directly north of the measurement site but covered wider areas also to the west and east. However, there were also some clear-cutting areas south and southeast of the measurements site.

2.2 Instrumentation

All instruments were set up in a temperature-controlled measurement container (~298 K) located at the sampling site. All sampling inlets were located 3.7 m above ground level and 1

https://doi.org/10.5194/egusphere-2024-1768
Preprint. Discussion started: 1 July 2024

m above the container roof. An overview of instruments and parameters measured is given in **Table S1**.

A PTR-ToF-MS 4000X2 coupled with a CHARON particle inlet (Ionicon Analytik GmbH, Innsbruck, Austria) was deployed to measure the VOCs and aerosol particles from 5th-30th of June 2020. A detailed description of the PTR-ToF-MS and CHARON inlet has been provided elsewhere (Jordan et al., 2009; Muller et al., 2017; Eichler et al., 2015). Briefly, CHARON consists of a charcoal denuder for stripping off gaseous organics, an aerodynamic lens for enriching particles, and a thermo-desorption unit (TDU) for particle evaporation prior to chemical analysis by PTR-ToF-MS. In this campaign, both gases and particles were measured through alternatingly switching between different modes with the data acquisition software (IoniTOF 4.0, Ionicon Analytik GmbH, Innsbruck, Austria). Specifically, one alternating measurement cycle includes 3-min HEPA filter mode for measuring the particle background, 1-min transition mode for the instrument equilibrium, 10-min CHARON mode for measuring particle phase compounds, another 1-min transition mode and 10-min VOC mode for measuring gas phase compounds (**Fig. S1**). One minute transition time is sufficient for the equilibrium of instrumental conditions between different modes (Piel et al., 2021). During the gas-phase measurement, ambient air was sampled continuously from a 3 m long PFA tube with a total flowrate of 1.45 L min^{-1}, and then a subset flow of ~0.1 L min^{-1} was sampled by the PTR-MS through a polyetheretherketone (PEEK) tubing maintained at 80 °C. During the particle-phase measurement, ambient particles were sampled by a $PM_{2.5}$ inlet with a flowrate of 16.7 L min^{-1}, out of which a flow of 0.55 L min^{-1} was directed to the CHARON inlet maintained by a vacuum pump (ACP15, Pfeiffer Vacuum). During a first measurement stage from 5th-19th of June, the PTR drift tube was set with alternating temperatures for gas and particle phase measurement modes at 80 °C and 120 °C respectively. With this setting, the actual drift tube temperatures were varying during the gas and particle measurement modes complicating the data analysis (**Figs. S1 and S2**). During a second measurement stage from 22nd-30th of June, the PTR drift tube was set with the same temperature of 120 °C and a drift tube pressure of 2.7 mbar for both gas and particle measurement modes. The CHARON inlet was set to a TDU temperature of 150 °C and a pressure of 7-8 mbar. Finally, the electric field (E/N) of the CHARON-PTR-TOF-MS was kept at ~97 Td and ~57 Td for the gas and particle phase measurement modes respectively during the second measurement stage (**Fig. S1b**). Gas calibrations of CHARON-PTR-TOF-MS were performed via dynamic dilution of a calibration gas cylinder containing 11 VOC species (**Table S2**, accuracy 10% at ~100 ppb). The background of VOCs was taken from zero-air measurements during the gas calibrations at the beginning and the end of the campaign. The

https://doi.org/10.5194/egusphere-2024-1768
Preprint. Discussion started: 1 July 2024

enrichment factor of the CHARON inlet was determined using an external calibration with size-selected ammonium nitrate particles (NH_4NO_3) that were counted using a condensation particle counter (CPC3772, TSI Inc., Shoreview, MN, USA). The enrichment factor was determined with an average value of 18 ± 2 in the 150-700 nm particle size range, with lower values for smaller particles below 150 nm (**Fig. S3**). The particle background was determined by a high-efficiency HEPA filter (ETA filter model HC01-5N-B, Aerocolloid LLC, Minneapolis, MN, USA) that was placed upstream of the gas-phase denuder of the CHARON inlet. All data files recorded by the CHARON-PTR-TOF-MS were processed by the software IONICON Data Analyzer (IDA version1.0.0.2, Ionicon Analytik GmbH, Innsbruck, Austria). More details of data processing with the IDA are given in **Supplement S1**. Please note that during the first measurement stage the actual temperature of the drift tube was fluctuating and hence lower than the intended temperature (120 °C, **Fig. S1**), which made it difficult to quantify particulate organic compounds. For the gas phase measurements, we corrected major VOC data during the first measurement stage based on the gas calibration and the cross-comparison with Vocus-PTR-ToF-MS measurements as described in **Supplement S2**. Finally, we can present the major VOC species measured by the CHARON-PTR-ToF-MS for the entire campaign, while the particle phase data for first measurement stage were excluded in this study.

A Vocus-PTR-ToF-MS (Aerodyne Research Inc., Billerica, MA, USA) was deployed to measure VOCs and oxygenated VOCs concurrently with the CHARON-PTR-ToF-MS from 10^{th}-30^{th} of June. The details of the Vocus-PTR-ToF-MS have been described elsewhere (Krechmer et al., 2018). The Vocus-PTR-ToF-MS is characterized by a newly designed reagent-ion source and a focusing ion-molecule reactor (FIMR), both of which improve the detection efficiency of ions. In this study, the FIMR was operated at a pressure of 1.5 mbar. The mass resolving power of the Vocus mass analyzer was ~10000 amu/Δamu. Raw data were recorded with a time resolution of 5 s. For the Vocus-PTR-ToF-MS measurement, ambient air was drawn in through a 1 m long PFA tubing with a total flow rate of 4.5 L min^{-1}, and then a subset flow of 0.1-0.15 L min^{-1} went into the Vocus-PTR-ToF-MS. Background measurements using high-purity nitrogen were automatically performed every hour. The Vocus-PTR-ToF-MS was regularly calibrated using a home-made gas standard of 15 compounds at ~1 ppmv with accuracy of 10% (**Table S2**). At the end of the campaign, a gas cross calibration was performed between Vocus-PTR-ToF-MS and CHARON-PTR-ToF-MS with the calibration gas cylinder (Ionicon Analytik GmbH). The Vocus-PTR-ToF-MS data analysis was performed using the software package "Tofware" (AG, Thun, Switzerland). For the quantification of uncalibrated species measured by the Vocus-PTR-ToF-MS, we adopted the rate constants of proton transfer

https://doi.org/10.5194/egusphere-2024-1768
Preprint. Discussion started: 1 July 2024

reactions (K_{cap}) from the PTR library (Pagonis et al., 2019). We then generated a sensitivity for the uncalibrated masses by applying a correction factor based on the k_{cap} ratios to the calibrated masses. Finally, the Vocus-PTR-ToF-MS data were synchronized to the measurement time of CHARON-PTR-ToF-MS for comparison of the VOC data.

In addition, methane (CH_4), carbon dioxide (CO_2), water vapor (H_2O) and carbon monoxide (CO) were measured with a cavity ring-down spectrometer (G2401; Picarro, Santa Clara, CA, USA) from 10th-30th of June. O_3 was measured by a commercial chemiluminescence analyzer (Cranox II, Eco Physics GmbH, Hürth, Germany). An optical particle counter (OPC, Fidas200, Palas, Karlsruhe, Germnay) was used to measure the mass concentrations of $PM_{2.5}$ and PM_{10} from 5th-30th of June. Simultaneously, black carbon (BC) concentrations were measured with an aethalometer (MA200, AethLabs, CA, USA). Particle number concentrations were measured with a condensation particle counter (CPC3776, TSI Inc., Shoreview, MN, USA). A nanoparticle sizer (NanoScan SMPS, TSI3910, TSI Inc., Shoreview, MN, USA) was used to measure the particle number size distribution between 10-410 nm.

Meteorological parameters were measured by a compact sensor (WS700, Lufft GmbH, Fellbach, Germany). The meteorological data were missing during some short periods due to the multifunction of data acquisition. We also used hourly data of temperature, relative humidity, precipitation, and boundary layer height from the European Centre for Medium-Range Weather Forecasts ERA5 reanalysis (Hersbach et al., 2020), as well as wind speed and direction data form NASA Power Data Access Viewer (power.larc.nasa.gov) to complement the meteorological data (**Fig. S4**). Besides, the daily soil moisture was measured by a Cosmic-Ray Neutron Sensor (CRNS) (Bogena et al., 2015), which was located ~150 m southwest of the sampling site.

2.3 Positive matrix factorization (PMF) analysis

The PMF receptor model is a bilinear analytic algorithm that separates the time series of air pollutants to different sources represented by factor profiles, factor time series and residual signals (Paatero and Tapper, 1994). The PMF model has been widely used to determine different sources and chemical processes of non-methane VOCs in the atmosphere (Gkatzelis et al., 2021; Li et al., 2021a; Wang et al., 2020; Li et al., 2022; Yuan et al., 2012; Pernov et al., 2021). To explore the sources and chemical processes of non-methane VOCs, we performed the PMF analysis of VOC species measured by the Vocus-PTR-ToF-MS rather than those measured by CHARON-PTR-ToF-MS. This is mainly due to the Vocus-PTR-ToF-MS can

https://doi.org/10.5194/egusphere-2024-1768
Preprint. Discussion started: 1 July 2024

measure higher molecular weight OVOCs (*mz*> 200) well that provides more information for interpreting the oxidation processes of BVOCs (Li et al., 2021a).

In this study, the Vocus-PTR-ToF-MS-measured VOC ions with a chemical formula assignment (mainly $C_xH_y^+$ and $C_xH_yO_z^+$) were selected to perform the PMF analysis. The PMF input data was further prepared according to the protocol reported in previous studies (Pernov et al., 2021; Li et al., 2022). Firstly, the concentrations of a VOC ion below the limit of detection (LOD) were replaced with half of the LOD and the associated uncertainties were set to 5/6 of the LOD. Missing concentrations of a VOC species were replaced with its median value during the campaign, and the corresponding uncertainties were set as values equal to 3 times the LOD. Furthermore, we excluded the VOC species into the PMF analysis if their concentration data are significantly below LOD or missing (> 20%). For example, we excluded $C_4H_9^+$ for the input of PMF analysis due to missing data during a significant fraction of the measurement period (**Fig. S5**). Furthermore, $C_4H_9^+$ measured by the Vocus-PTR-ToF-MS cannot provide more source information because it can be related to biogenic or anthropogenic sources and fragmentation of many VOCs like alcohols and aldehydes (Li et al., 2020). Finally, 157 VOC ions measured by the Vocus-PTR-ToF-MS were chosen for the PMF analysis (**Table S3**). The sum concentrations of 157 VOC ions measured by the Vocus-PTR-ToF-MS showed a good agreement with the sum concentrations of major VOCs measured by the CHARON-PTR-ToF-MS (**Fig. S5**). Therefore, the solution of PMF analysis on these 157 VOC ions measured by the Vocus-PTR-ToF-MS can reasonably interpret the major sources and/or chemical processes of non-methane VOCs in this study. The PMF analysis was performed using the PMF Evaluation Tool (v3.05) that runs in IGOR Pro software (v6.37, Wavemetrics, Portland, OR). The summary of diagnostic plots for the PMF solution is given in **Fig. S6**.

3 Results and discussion

In the first section we will give an overview of the measurements conducted and in the second section we will address the impacts of meteorological factors like wind speed and direction, temperature, and relative humidity on the variations of gas and particle concentrations. In the third section we perform a source apportionment of the non-methane VOCs observed, and in the last section we discuss BVOC oxidation products in gas and particle phase.

3.1 Overview of the measurements

During the entire campaign, the average ambient temperature and relative humidity (RH) were 16.6 ± 4.7 °C and 71% ± 16% respectively (**Fig. 1**). The wind speeds ranged from 0-5.5

https://doi.org/10.5194/egusphere-2024-1768
Preprint. Discussion started: 1 July 2024

m s^{-1} with an average of 1.3 ± 0.9 m s^{-1}. Wind directions varied significantly during the entire measurement period. The sampling site was potentially affected by BPP-related and/or anthropogenic emissions for westerly to northwesterly wind directions (**Fig. 1a**). Two characteristic episodes: Episode 1 (0:00 9th of June to 0:00 12th of June) and Episode 2 (12:00 23rd of June to12:00 26th of June) were observed for their distinctly different meteorological conditions. Episode 1 had lower temperatures with an average of 12.9 ± 1.7 °C compared to Episode 2 with 23.0 ± 4.2 °C, thus hereafter we define them as low-T and high-T episodes, respectively. Both episodes had very low wind speeds (< 1 m s^{-1}, **Fig. 1b**), suggesting the site was influenced by local emissions and chemical transformation or aging processes. The impacts of meteorology and chemical processes on the variations of gases and particles will be discussed in the following sections.

As shown in **Fig. 2**, the average concentrations of CO and CO_2 were 0.11 ± 0.02 ppm and 410 ± 1 ppm respectively from 10th-30th of June. The concentration of CH_4 ranged from 1.90 to 2.56 ppm with an average of 1.98 ± 0.05 ppm. Spikes of CH_4 (> 2.2 ppm) were occasionally observed during the days of 17, 20-21 and 23 June, which are associated with BPP-related emissions as validated in Section 3.2. Isoprene and monoterpenes were quantitatively measured by the CHARON-PTR-ToF-MS and Vocus-PTR-ToF-MS with good agreements. During the entire campaign, the average concentration of isoprene was 0.58 ± 0.54 ppb, comparable to that (~0.6 ppb) observed in French Landes forest (Li et al., 2020) but higher than in the boreal forests (0.01-0.2 ppb) during summertime (Li et al., 2021a; Hellén et al., 2018). The average concentration of monoterpenes was 2.5 ± 5.3 ppb, lower than those observed in the French Landes forest (~6 ppb) with a higher density of monoterpene-emitting tree species (Li et al., 2020). Relatively low concentrations of monoterpenes were reported previously in boreal forests (~0.8 ppb) during summertime (Li et al., 2020; Mermet et al., 2021). Note that monoterpenes had a significant concentration variation in this study, which is attributed to the occurrence of monoterpene spikes (**Fig. 2d**). These monoterpene spikes were mainly related to the impact of BPP-related emissions as discussed in section 3.2. In this study, the average concentration of sesquiterpenes measured by the CHARON-PTR-ToF-MS was 0.01 ± 0.01 ppb, a factor of two higher than that measured by the Vocus-PTR-ToF-MS. The average concentration of sesquiterpenes was lower than that measured by a Vocus-PTR-ToF-MS in the Landes forest (~0.06 ppb) (Li et al., 2020). The degree of sesquiterpene fragmentation can be significantly different for various PTR-ToF-MS depending on the instrument setting (Kim et al., 2009; Kari et al., 2018). Due to a lack of a dedicated sesquiterpene calibration in this study, the concentrations of sesquiterpenes measured by the CHARON-PTR-ToF-MS or Vocus-PTR-

https://doi.org/10.5194/egusphere-2024-1768
Preprint. Discussion started: 1 July 2024

ToF-MS can be regarded as the lower limit without the consideration of fragmentation. Besides, a series of VOC species were simultaneously detected by the CHARON-PTR-TOF-MS and Vocus-PTR-ToF-MS and a detailed comparison is presented in **Supplement S2**.

During the entire campaign, the average mass concentrations of $PM_{2.5}$ and BC were 5.5 ± 4.7 μg m^{-3} and 0.2 ± 0.1 μg m^{-3} respectively (**Fig. S7**). The aerosol particle composition including organic aerosol (OA), nitrate, and ammonium measured by the CHARON-PTR-ToF-MS and BC by the aethalometer are simultaneously available from 22nd-30th of June (**Fig. 3**). During this period, the average mass concentrations of OA was 0.8 ± 0.5 μg m^{-3}, accounting for 15 ± 6 % of $PM_{2.5}$ mass. The mass fraction of CHARON-PTR-ToF-MS-measured OA in $PM_{2.5}$ was close to that of semi-volatile oxygenated OA (SV-OOA) in $PM_{2.5}$ (9%-13%) resolved from the PMF analysis of OA measured by an aerosol mass spectrometer (AMS) in urban and rural environments (Song et al., 2022; Huang et al., 2019). The elemental ratios of OA (O:C and H:C) measured by the CHARON-PTR-ToF-MS were 0.32 ± 0.03 and 1.56 ± 0.10, respectively, which are comparable to the values of SV-OOA (O:C: 0.35 ± 0.14 and H:C: 1.55 ± 0.10) resolved from the AMS-PMF analysis in previous studies (Ng et al., 2011; Ng et al., 2010). These results indicate that the OA mass detected by the CHARON-PTR-ToF-MS is mainly composed of semi-volatile organic compounds in this study. Mass concentrations of OA associated with individual *m/z* signals detected by the CHARON-PTR-ToF-MS ranged from ~0.1 to ~65 ng m^{-3}. In total, 164 organic ions can be well assigned with the chemical formula of $C_xH_y^+$ or $C_xH_yO_z^+$, contributing to 67 ± 11 % of total OA mass measured by the CHARON-PTR-ToF-MS. Furthermore, the organic ions assigned were mainly distributed in the C_2-C_{10} range with oxygen atom numbers of 0-5 (**Fig. 3d**). Müller et al., (2017) observed a similar mass distribution of OA measured by the CHARON-PTR-ToF-MS in Valencia, Spain which was associated with the oxidation of abundant monoterpenes emitted from trees. With the same instrument, Gkatzelis et al., (2018) also reported a similar chemical composition of OA from the oxidation of tree emissions dominated by α-pinene and β-pinene in simulation chamber experiments. The abundant species in the C_2-C_8 range (**Fig. 3d**) are most likely fragments from $C_{9\text{-}10}$-monoterpene derived oxidized products which are prone to fragmentation in the CHARON-PTR-ToF-MS (Gkatzelis et al., 2018). Leglise et al., (2019) and Peng et al., (2023) further confirm the fragmentation of oxygenated organic compounds inside the CHARON-PTR-ToF-MS via the loss of neutral water, carbonyl, or carboxyl groups (-H_2O, -CO and -CO_2). For instance, *cis*-pinonic acid ($C_{10}H_{17}O_3^+$) a monoterpene oxidation product as detected by the CHARON-PTR-ToF-MS can produce the typical fragment ions of $C_4H_7O^+$, $C_6H_{11}O_2$+ and $C_{10}H_{15}O_2^+$ (Peng et al., 2023; Leglise et al., 2019). Furthermore, the relative abundance of

https://doi.org/10.5194/egusphere-2024-1768
Preprint. Discussion started: 1 July 2024

fragment ions ($C_4H_7O^+$, $C_6H_{11}O_2$+ and $C_{10}H_{15}O_2^+$) were generally higher than the parent ion $C_{10}H_{17}O_3^+$ (Leglise et al., 2019; Peng et al., 2023). In this study, we found that only a small fraction of the *cis*-pinonic acid parent ion $C_{10}H_{17}O_3^+$ was detected by the CHARON-PTR-ToF-MS compared to the fragment ions $C_4H_7O^+$, $C_6H_{11}O_2^+$ and $C_{10}H_{15}O_2^+$ (**Fig. S8**). Similarly, other monoterpene oxidation products such as $C_9H_{15}O_3^+$ (e.g., norpinonic acid) and $C_8H_{13}O_4^+$ (e.g., norpinic acid) showed lower abundances at their parent ions compared to their fragment ions with one H_2O molecule lost ($C_9H_{13}O_2^+$ and $C_8H_{11}O_3^+$). The fragmentation pattern of oxidized organic compounds in the CHARON-PTR-ToF-MS varied depending on the instrument settings (Leglise et al., 2019), therefore we cannot compare the fragmentation patterns of organic compounds from our instruments with those from other studies. However, it is consistent with other studies that the particulate oxidized organic compounds measured by the CHARON-PTR-ToF-MS in this study were mainly detected as the more abundant fragment ions after losing one H_2O molecule rather than as the parent ions.

3.2 Meteorological impacts on the variations of VOCs

We firstly analyzed the variations of gas and particle concentrations as a function of wind direction (WD) with a bin of 10° (**Fig. 4**). During the entire measurement period, the sampling site was influenced by the WD varying from 0-330°. Within the WD sectors of 0-240°, 240-300° and 300-330°, the site was influenced by the winds coming from the forest, the BPP and the village residential areas respectively (**Fig. 1**). We found that the concentrations of CH_4 increased significantly in the WD sector of 240-300° and remained high concentrations in the WD sector of 300-330°. In contrast, constantly low concentrations of CH_4 were observed when the site was influenced by the WD sector of 0-240° from the forest. For the WD sectors of 240-300° and 300-330°, both wind speeds and the PBL heights were decreased. This indicates that the increase in CH_4 concentration was also related to the accumulation of anthropogenic emissions from the BPP and/or village residential areas under stagnant meteorological conditions. In the WD sector of 240-300°, we also observed a significant increase of monoterpenes concentrations. The ambient temperature was constantly low (~15 °C) at the WD sector of 240-300°. It suggests that the increase of monoterpene concentrations in the WD sector of 240-300° was attributed to BPP-related emissions rather than biogenic emissions induced by high temperatures. In contrast to CH_4, monoterpenes showed very low values in the WD sector of 300-330°, suggesting a minor impact of anthropogenic emissions from the village residential areas on monoterpene concentrations.

https://doi.org/10.5194/egusphere-2024-1768
Preprint. Discussion started: 1 July 2024

Fig. S9 shows the high-time resolution (minutes) measurement data for several cases with rapid increases of monoterpene or CH_4 concentrations. For example, during 18:00-21:00 on 8th of June, the WD shifted from the forest areas (60-120°) to the BPP (240-270°). Correspondingly, monoterpene and sesquiterpene concentrations showed rapid increases. Subsequently, during 21:00 on 8th of June to 01:00 on 9th of June, the winds were constantly coming from a direction of ~270-300°, the concentrations of monoterpenes and sesquiterpenes dropped down to low values. Similarly, during 00:00-03:00 and 21:00-24:00 on 20th of June, low concentrations of monoterpenes and sesquiterpenes were observed when the wind direction was constantly coming from the direction of ~300-330°. In contrast, a significant increase of CH_4 concentration was observed during 00:00-03:00 and 21:00-24:00 on 20th of June, when the sampling site was influenced by the WD sector of ~270-330°. Note that the biowaste storage and fermentation tank of the BPP were located in the WD sector of 240-270° (**Fig. 1a**), while the biogas storage tank was specifically located in the WD sector of 270-300 º. Therefore, the rapid increase of CH_4 concentrations could related to the leak of CH_4 from the BPP in the WD sector of 270-300° or the anthropogenic emissions in the WD sector of 300-330°. However, the rapid increase of monoterpene concentrations at the WD of 240-270 º was associated with the emissions from the biowaste storage and fermentation tank of the BPP. In addition, significant variations of isoprene, monoterpene and sesquiterpene concentrations were observed at the WD sector of 0-240°, which were associated with the changes of biogenic emissions and/or chemical transformation processes. Note that the highest concentrations of CO, CO_2, BC and $PM_{2.5}$ were observed in the WD sector of 0-60°, and were caused by the stagnant meteorological conditions with low wind speed (WS) and PBL height.

Based on the above wind direction analyses, we classified the meteorological, gas and particle measurement data into two major groups influenced by the WD sector of 240-330° from the BPP (WD-BPP) and the WD sector of 0-240° from the forest (WD-forest), respectively. During some short periods, meteorological data were missing due to the malfunction of instrument data acquisition. We excluded the gas and particle data for the classification based on wind direction analyses during these short periods when the meteorological data were not measured. **Figure 5** shows the diurnal variations of meteorological parameters as well as gas and particle species calculated for the groups of WD-BPP and WD-forest, respectively. In the WD-BPP group, the diurnal variations of CH_4 concentrations showed higher concentrations during nighttime, which were related to the BPP emissions, low wind speed and PBL height. The diurnal behavior of monoterpene concentrations in the WD-BPP group showed higher average values during nighttime but with

https://doi.org/10.5194/egusphere-2024-1768
Preprint. Discussion started: 1 July 2024

large fluctuations over the whole day. These fluctuations with spikes in monoterpene concentrations were related to the contribution of BPP emissions depending on the wind directions. In the WD-forest group, CH_4 concentrations showed less pronounced diurnal variations. Isoprene showed higher concentrations during daytime in the WD-forest group, which is similar to the diurnal behavior of isoprene in previous observations in forests (Yáñez-Serrano et al., 2015; Hakola et al., 2012; Li et al., 2020). This is mainly due to higher temperatures and intensive radiation during daytime. In the WD-forest group, the diurnal variations of monoterpene and sesquiterpene concentrations showed very low valuesduring daytime due to the expanding PBL and strong photochemical consumption. The concentrations of monoterpenes and sesquiterpenes peaked at ~18:00 when the concentrations of atmospheric oxidants (OH radicals and O_3) and PBL heights decreased. Monoterpenes and sesquiterpenes showed low concentrations with <1 ppb and <0.01 ppb after 18:00 during nighttime in the WD-forest group. This is different with previous studies where constantly higher concentrations of monoterpenes and sesquiterpenes but lower O_3 concentrations (<20 ppb) were observed during nighttime compared to daytime (Hakola et al., 2012; Li et al., 2020). However, in our study, higher O_3 concentrations (~30 ppb) were observed during nighttime in the WD-forest group, which may have reduced the concentrations of monoterpenes and sesquiterpenes by nighttime oxidation.

Note that the concentrations of monoterpenes and sesquiterpenes were low during daytime, but they increased slightly from 8:00-12:00 when the temperature and radiation increased. **Figure 6** shows the time series of isoprene, monoterpenes, sesquiterpenes and O_3 along with wind direction and ambient temperature during low-T and high-T episodes. During daytime of the high-T episode, we observed that the concentrations of isoprene, monoterpenes, sesquiterpenes all increased as the temperature increased when the sampling site was constantly influenced by the WD of ~100° from the forest. Meanwhile, constantly high concentrations of O_3 (40-60 ppb) were observed during daytime of the high-T episode. This suggests that increasing biogenic emissions due to higher temperatures exceeded the photochemical consumptions. Similarly, higher concentrations of O_3 were observed during daytime of the low-T episode when the sampling site was also constantly influenced by the wind direction of ~100° (e.g., 11th of June). However, the concentrations of isoprene, monoterpenes, sesquiterpenes showed no increase. In **Fig. 6a**, we also found that very high concentrations of monoterpenes and sesquiterpenes during the low-T episode (e.g., 20:00-24:00, 10th of June) were associated with the changes of wind directions, which was in line with the wind direction analyses as discussed above. Soil moisture showed no significant difference between the low-T and high-

https://doi.org/10.5194/egusphere-2024-1768
Preprint. Discussion started: 1 July 2024

T episode (**Fig. S4**), indicating that it had only a minor or no impact on the variations of BVOC concentrations.

3.3 Source apportionment of VOCs

In addition to meteorological impacts, the variations of VOC concentrations are influenced by different emission sources and chemical processes. We performed a PMF analysis of Vocus-PTR-ToF-MS-measured non-methane VOC data to identify and determine the impacts of different sources and oxidation processes. According to the factor profiles, temporal variations, and correlation analysis with tracer ions, we present a six-factor solution where VOCs are apportioned to (1) terpenes, (2) daytime-biogenic OVOC, (3) nighttime-biogenic OVOC (4) aromatic OVOC (5) organic acid-1 and (6) organic acid-2. **Figure 7** shows the factor profiles, time series and diurnal variations of six factors during the entire measurement campaign.

The first factor profile was dominated by the monoterpenes ($C_{10}H_{17}^+$) and its fragment ions ($C_6H_9^+$ and $C_7H_{11}^+$) (Tani et al., 2003; Kari et al., 2018), thus we defined it as a factor of terpenes. Correspondingly, the time series of this factor highly correlated with monoterpene-related ions including $C_6H_9^+$ $C_7H_{11}^+$ and $C_{10}H_{17}^+$ as well as $C_{10}H_{19}O^+$ ($r > 0.9$, **Fig. S10**). $C_{10}H_{19}O^+$ can be assigned as a terpene alcohol e.g., linalool (Li et al., 2020), which can be emitted by leaves and flowers directly (Joó et al., 2010). As discussed before, the variations of monoterpene concentrations were influenced by the BPP emissions and biogenic emissions depending on the wind directions. In this study, PMF analysis could not separate the relative contribution of biogenic emissions and BPP emissions to monoterpenes directly. Based on wind direction analyses, monoterpenes were expected to be mainly emitted by the trees when the winds were coming from the forest regions.

Two OVOC factors representing oxidation processes of BVOCs during nighttime and daytime (nighttime-biogenic OVOC and daytime-biogenic OVOC), respectively, were resolved from the PMF analysis. The factor profile of nighttime-biogenic OVOC was characterized with high fractions of $C_9H_{15}O^+$ (nopinone), $C_{10}H_{17}O^+$ (monoterpene oxide), $C_{10}H_{17}O_2^+$ and $C_{10}H_{15}O^+$ (pinonaldehyde fragment ion), which are weakly-oxidized products of monoterpenes with oxygen atom number < 3 (Li et al., 2021a; Li et al., 2020; Vermeuel et al., 2023). The diurnal pattern of the nighttime-biogenic OVOC factor showed higher concentrations at nighttime. As shown in **Fig. S10**, the time series of the nighttime-biogenic OVOC well correlated with $C_{10}H_{15}O^+$ ($r = 0.68$) and $C_{10}H_{17}O_2^+$ ($r = 0.65$). Li et al., (2021a) performed a binPMF analysis on Vocus-PTR-MS-measured VOC data at two European forest sites. They also resolved a factor representing weakly-oxidized products of monoterpenes with higher concentrations at

https://doi.org/10.5194/egusphere-2024-1768
Preprint. Discussion started: 1 July 2024

night (Li et al., 2021a). In this study, the factor profile of daytime-biogenic OVOC was characterized with high fractions of isoprene and its oxidation products (e.g., $C_5H_9^+$, $C_4H_7O_{1-4}^+$ and $C_5H_9O_{2-4}^+$) as well as stronger oxidized products of monoterpenes with oxygen atom number >3 (e.g., $C_{10}H_{17}O_{4-5}^+$). In contrast to nighttime-biogenic OVOC factor, the time series of the daytime-biogenic OVOC factor correlated well with a suite of more-oxidized species with oxygen atom number >2 (**Fig. S10**). In particular, the time series of the daytime-biogenic OVOC factor showed good correlations with isoprene oxidation products $C_5H_9O_{2-4}^+$ (r = 0.66-0.80) and more-oxidized monoterpene products e.g., $C_9H_{15}O_5^+$ and $C_{10}H_{17}O_5^+$ (r > 0.60). The diurnal variation of the daytime-biogenic OVOC factor showed higher concentrations during daytime. Li et al., (2021a) resolved one factor representing isoprene and its oxidation products and another factor representing stronger oxidized products of monoterpenes from the binPMF analysis for a low-mass (*mz*50-200) and a high-mass range (*mz*201-320), respectively, for two European forest sites. They found that these two factors had a similar diurnal pattern with high daytime concentrations. In our study, we performed the PMF analysis for the full mass range (mz40-220) of the major VOC ions and resolved one factor of daytime-biogenic OVOCs. It suggests that isoprene oxidation products and stronger oxidized products of monoterpenes were mainly related to the daytime oxidation processes.

The fourth factor was characterized as aromatic OVOC with high fractions of $C_6H_7O^+$ (phenol), $C_6H_7O_2^+$ (catechol), and $C_7H_7O_2^+$ (benzoic acid) in its factor profile (**Fig. 7**). These OVOC species originate from the oxidation of aromatic hydrocarbons (Hamilton et al., 2005; Zaytsev et al., 2019; Li et al., 2021b; Wu et al., 2014; Lannuque et al., 2023). As shown in **Fig. S10**, good correlations were found for aromatic OVOC with catechol (r = 0.87 for $C_6H_7O_2^+$) and benzoic acid (r = 0.84 for $C_7H_7O_2^+$). In addition, the factor of aromatic OVOC also correlated well (r = 0.77-0.87) with $C_5H_5O_3^+$ (e.g., methylfurandione), $C_5H_5O_2^+$ (e.g., butenedial), $C_4H_5O_2^+$ (e.g., furfural), and $C_3H_5O_2^+$ (e.g., methylglyoxal). These compounds are likely ring-opening products of toluene oxidation as reported in previous studies (Zaytsev et al., 2019; Wu et al., 2014; Lannuque et al., 2023). The diurnal variation of aromatic OVOC showed slightly higher concentrations during daytime, which can be related to an enhanced photochemical oxidation of aromatic hydrocarbons.

The fifth and sixth VOC factors were associated with gaseous organic acids. Specifically, the fifth factor profile had high fractions of $C_2H_5O_2^+$ and $C_2H_7O_3^+$, which can be assigned as acetic acid and its water cluster respectively. High fractions of $C_3H_7O_2^+$ and $C_4H_9O_2^+$ were also found in the fifth factor profile, which can be assigned as propionic acid and butyric acid,

https://doi.org/10.5194/egusphere-2024-1768
Preprint. Discussion started: 1 July 2024

484 respectively. The sixth factor profile showed high fractions of $C_2H_5O_2^+$ (acetic acid), $C_3H_9O_2^+$
485 (e.g., propylene glycol) and $C_4H_7O_4^+$ (e.g., succinic acid). Therefore, the fifth and sixth factor
486 were defined as organic acid-1 and organic acid-2, respectively. As shown in **Fig. S10**, the time
487 series of organic acid-1 showed the highest correlations with acetic acid-related ions $C_2H_7O_3^+$
488 (r = 0.79) and $C_2H_5O_2^+$ (r = 0.63) as well as $C_3H_9O_3^+$, which was assigned as the water cluster
489 ion of propionic acid ($C_3H_7O_2^+$). The time series of organic acid-2 showed strong correlations
490 with $C_4H_6O^+$ (r = 0.90, **Fig. S10**) and $C_2H_5O_3^+$ (r = 0.89), which can be assigned as the isoprene
491 oxidation product as deprotonated $C_4H_7O^+$ (MVK+MACR) and glycolic acid, respectively. In
492 addition, O_3 was only weakly correlated with organic acid-1 (r = 0.27), but much better
493 correlated with organic acid-2 (r = 0.57). Moreover, a better correlation was found between O_3
494 and the sum of these two organic acid factors (r = 0.70). The diurnal variations of both organic
495 acid factors showed higher concentrations during daytime. These results suggest that both
496 organic acid factors are related to the daytime photooxidation of BVOCs.

497 As shown in **Fig. 8a**, the total concentration of non-methane VOCs measured by the Vocus-
498 PTR-ToF-MS for the PMF analysis was 9.0 ± 4.4 ppb during the entire campaign. The
499 concentration of total non-methane VOCs (TVOCs) was dominated by the two organic acid
500 factors with 27% ± 20% and 18% ± 21% from organic acid-1 and organic acid-2, respectively,
501 followed by the nighttime-biogenic OVOCs (17% ± 15 %). This indicates substantial
502 contributions of oxygenated species to TVOCs during the entire campaign. Based on the wind
503 direction analysis, we further compared the relative contributions of VOC factors to TVOCs for
504 the groups of WD-forest and WD-BPP. The average concentration of TVOCs in the WD-forest
505 group (9.7 ± 4.7 ppb) were slightly higher than that in the WD-BPP group (7.1 ± 3.6 ppb). The
506 contribution of organic acid-1 to TVOCs was comparable with 25% ± 21% and 32% ± 18% for
507 the groups of WD-forest and WD-BPP, respectively. However, the contribution of organic acid-
508 2 to TVOCs in the WD-forest group (26% ± 25%) was higher than that in the WD-BPP group
509 (13% ± 15%). We observed elevated concentrations of organic acid-2 during the high-T episode
510 (23^{rd}-26^{th} of June, **Fig. 7b**). As mentioned before, the sampling site was mainly influenced by
511 the winds coming from the forest during high-T episode along with higher concentrations of
512 O_3. Therefore, higher contribution of organic acid-2 in the WD-forest group was attributed to
513 the strong oxidation of BVOCs. The contribution of terpenes to TVOCs was higher in the WD-
514 BPP group (18% ± 16%) compared to that in the WD-forest group (11% ± 15%). This is
515 consistent with the wind direction analyses that higher monoterpene concentrations were related
516 to BPP emissions. In addition, the contributions of nighttime-biogenic and daytime-biogenic
517 OVOC factors to TVOCs concentrations were slightly higher in the WD-BPP group, which

https://doi.org/10.5194/egusphere-2024-1768
Preprint. Discussion started: 1 July 2024

were related to high abundances of monoterpenes. Furthermore, gas-to-particle partitioning processes could also influence the variations of BVOC oxidation products and thus nighttime-biogenic and daytime-biogenic OVOC factors.

3.4 Variations of BVOC oxidation products in gas- and particle phases

Figure 9 shows the diurnal variations of concentrations of organic molecules ($C_5H_9O_{1\text{-}4}^+$, $C_4H_7O_{1\text{-}4}^+$, $C_{10}H_{17}O_{1\text{-}5}^+$ and $C_{10}H_{15}O_{1\text{-}5}^+$) in the gas phase measured by the Vocus-PTR-ToF-MS and particle phase compounds measured by the CHARON-PTR-TOF-MS during 22nd-30th of June. These organic molecules are important components of nighttime-biogenic and daytime-biogenic OVOC factors resolved by the PMF analysis, and they are identified as the oxidation products from isoprene and monoterpenes based on previous field observations and simulation chamber experiments (Gkatzelis et al., 2018; Li et al., 2020). For example, gaseous $C_4H_7O^+$ can be the sum of methyl vinyl ketone (MVK) and methacrolein (MACR), which are major products of the isoprene oxidation (Wennberg et al., 2018). $C_{10}H_{17}O_3^+$ can be attributed to *cis*-pinonic acid formed from the oxidation of monoterpenes (e.g., α-pinene). Again, the fragmentation of high-molecular weight oxidized organic compounds measured by the PTR-ToF-MS instruments could produce the fragment ions via the loss of neutral water, carbonyl, or carboxyl groups (-H_2O, -CO and -CO_2). The diurnal variations of all isoprene oxidation products ($C_5H_9O_{1\text{-}4}^+$ and $C_4H_7O_{1\text{-}4}^+$) in both gas and particle phases showed higher concentrations from morning (6:00-8:00) to afternoon (12:00-16:00) as well as isoprene itself. These results indicate that higher temperatures and intensive sunlight not only favor the isoprene emissions but also enhance photochemical oxidation of isoprene. Besides, we found that the concentrations of particulate $C_4H_7O_{1\text{-}2}^+$ showed increased values from early nighttime (18:00-20:00) to midnight (0:00-2:00 of the next day). As mentioned before, the fragmentation of *cis*-pinonic acid in the CHARON-PTR-ToF-MS can produce the fragment ions $C_4H_7O^+$, $C_6H_{11}O_2$+ and $C_{10}H_{15}O_2^+$ (Gkatzelis et al., 2018; Peng et al., 2023; Muller et al., 2017; Leglise et al., 2019). Furthermore, we observed a similar diurnal pattern of $C_4H_7O^+$and $C_{10}H_{15}O_2^+$ in the particle phase, suggesting that the nighttime increase of particulate $C_4H_7O^+$ was likely contributed by the fragmentation of *cis*-pinonic acid. Due to instrumental limitation, it is difficult to assign each ion detected by the PTR-ToF-MS to either parent ion or fragment ion of one organic compound in the ambient particles.

The diurnal variations of weakly-oxidized products of monoterpenes like $C_{10}H_{17}O_{1\text{-}2}^+$ and $C_{10}H_{15}O_{1\text{-}2}^+$ in both gas and particle phases showed elevated concentrations during nighttime. In contrast, the more-oxidized products of monoterpenes ($C_{10}H_{17}O_{4\text{-}5}^+$ and $C_{10}H_{15}O_{4\text{-}5}^+$) showed

https://doi.org/10.5194/egusphere-2024-1768
Preprint. Discussion started: 1 July 2024

higher concentrations in gas and particle phases during daytime. The higher atmospheric oxidation capacity during daytime compared to nighttime leads to the formation of more-oxidized products. In addition, $C_{10}H_{17}O_3^+$ (*cis*-pinonic acid) and its fragment ion ($C_{10}H_{15}O_2^+$) in the gas phase showed less pronounced diurnal patterns. The particulate $C_{10}H_{17}O_3^+$ also showed a less pronounced diurnal behavior, while the particulate $C_{10}H_{15}O_2^+$ showed increased concentrations during nighttime. This is in agreement with previous findings that most of the particulate compounds detected by the CHARON-PTR-ToF-MS were not detected as the parent ion but as the fragment ion with one H_2O molecule lost (Gkatzelis et al., 2018). In this study, $C_{14}H_{23}O_2^+$, $C_{15}H_{23}O^+$, $C_{15}H_{25}O_2^+$ were measured by the PTR instruments, which can be considered as the sesquiterpene oxidation products based on previous field and simulation chamber studies. Here $C_{14}H_{23}O_2^+$ was detected only in the gas phase by the Vocus-PTR-ToF-MS, while $C_{15}H_{23}O_2^+$ and $C_{15}H_{25}O_2^+$ were detected only in the particle phase by the CHARON-PTR-ToF-MS. The concentrations of sesquiterpene oxidation products in both gas (<0.5 ppt) and particle phases (<5 ng m^{-3}) were relatively low probably due to correspondingly low concentrations of sesquiterpenes in this study. The diurnal pattern of gaseous $C_{14}H_{23}O_2^+$ showed two peaks in the morning and early evening (**Fig. S11**), which was similar to those of weakly-oxidized products of sesquiterpenes (e.g., $C_{14}H_{22}O_{1\text{-}3}$ and $C_{15}H_{24}O_{1\text{-}3}$) observed at the Landes forest in France (Li et al., 2020). The diurnal variations of particulate $C_{15}H_{23}O_2^+$ and $C_{15}H_{25}O_2^+$ showed slightly higher values during nighttime.

Furthermore, we calculated the variations of OA/ΔCO, which are the total OA concentrations measured by the CHARON-PTR-ToF-MS normalized over ΔCO (subtracted by the background CO concentration) to exclude the impact of boundary layer height variations, during 22nd-30th of June (Fig. 10). An increase of OA/ΔCO was observed during nighttime of the high-T episode, which could be related to the gas-to-particle partitioning of monoterpene oxidation products. Here we calculated the particulate fraction (F_p) of monoterpene oxidation products by the following equation:

$$F_p = \frac{C_{p,i}}{C_{g,i} + C_{p,i}}$$

where $C_{p,i}$ and $C_{g,i}$ are the particle and gas phase concentrations of the species measured by CHARON-PTR-ToF-MS and Vocus-PTR-ToF-MS, respectively. Both gas and particle phase data of $C_{10}H_{17}O_{1\text{-}3}^+$ and $C_{10}H_{15}O_{1\text{-}5}^+$ are available for the F_p calculation in this study. The two PTR instruments used in this study may have different sensitivities or fragmentation for different oxygenated organic compounds. For example, the concentrations of monoterpene

https://doi.org/10.5194/egusphere-2024-1768
Preprint. Discussion started: 1 July 2024

oxidation products such as $C_9H_{15}O^+$, $C_{10}H_{15}O_{1\text{-}2}^+$ and $C_{10}H_{17}^+$ measured by the Vocus-PTR-ToF-MS were ~2-3 times higher than those measured by the CHARON-PTR-ToF-MS (**Fig. S13b**). Although we cannot precisely calculate the F_p values for each OA molecule due to instrumental limitations, the variations of calculated F_p values can still be used as an indicator for estimating the gas-to-particle portioning processes. As shown in **Fig. 10**, weakly-oxidized molecules of monoterpenes ($C_{10}H_{17}O_{1\text{-}2}^+$ and $C_{10}H_{15}O_{1\text{-}3}^+$) had lower F_p values compared to more-oxidized molecules of monoterpenes ($C_{10}H_{17}O_3^+$ and $C_{10}H_{15}O_{4\text{-}5}^+$). This is expected because more-oxidized products of monoterpenes generally have lower volatility compared to weakly-oxidized ones. Interestingly, the F_p values of weakly-oxidized molecules of monoterpenes showed similar temporal trends as the relative humidity. Especially for the high-T episode, the F_p values of weakly-oxidized molecules of monoterpenes ($C_{10}H_{15}O_{1\text{-}3}^+$) showed positive correlations (r = 0.65-0.71) with RH. This indicates that increasing RH can enhance the particle fraction of weakly-oxidized molecules of monoterpenes and thus increase SOA mass. As validated in Section 3.3, these weakly-oxidized molecules of monoterpenes are formed by oxidation of monoterpenes emitted from trees during the high-T episode rather than from BPP emissions. It is reasonable to assume that these monoterpenes are mainly α-pinene and β-pinene emitting from the Norway spruce and European beech trees at our sampling site. Previously, Tillmann et al., (2010) found that the SOA yields from the ozonolysis of α-pinene were higher at humid conditions than at dry conditions. More recently, Surdu et al., (2023) studied the effect of RH on the partitioning of oxidized organic molecules formed from α-pinene oxidation at the CERN CLOUD chamber. They observed that the particle-phase concentrations of semi-volatile organic molecules ($C_{10}H_{16}O_{2\text{-}3}$) from α-pinene oxidation significantly increases by factors of 2-4 with increasing RH, thus leading to a substantial increase of SOA mass (Surdu et al., 2023). Similarly, Luo et al., (2024) reported that increasing RH from 3% to 84% increase the abundance of less oxidized products (e.g., $C_{10}H_{16}O_{2\text{-}6}$) from α-pinene ozonolysis. In our study, during the high-T episode, we observed the F_p values for $C_{10}H_{15}O^+$, $C_{10}H_{15}O_2^+$ and $C_{10}H_{15}O_3^+$ increased by ~2%, ~6% and ~20% respectively when RH was increased from 30-40% to 60-80%. Besides, the ambient temperature was anticorrelated with RH in this study. Thus, lower temperatures may further additionally favor the gas-to-particle partitioning of semi-volatile organic molecules from monoterpene oxidation.

https://doi.org/10.5194/egusphere-2024-1768
Preprint. Discussion started: 1 July 2024

4 Conclusions

In this study, we investigated the characteristics of VOCs and OA particles simultaneously measured by a CHARON-PTR-ToF-MS and a Vocus-PTR-ToF-MS at a pine forest stressed by bark beetles and previous droughts close to a BPP in western Germany during June 2020. The average concentrations of isoprene, monoterpenes and sesquiterpenes were quantified and ranged within the values observed in other European forests during summertime (Mermet et al., 2021; Li et al., 2021a; Hellén et al., 2018). The average particle mass concentration of OA detected by the CHARON-PTR-ToF-MS was 0.8 ± 0.5 μg m^{-3} which mainly consisted of semi-volatile organic compounds formed from monoterpene oxidation. Based on a wind direction analyses, gas and particle measurement data were categorized into two groups to distinguish between emissions of a biogas power plant (WD-BPP) and the forest (WD-forest). The concentrations of CH_4 and also monoterpenes were larger in the WD-BPP group. This was expected for methane and it is also known that BPP can release high concentrations of monoterpenes during biowaste storage and fermentation processes (Salazar Gómez et al., 2016; Papurello et al., 2012). In the WD-forest group, the concentrations of isoprene, monoterpenes and sesquiterpenes showed the increases during daytime especially for the high-T episode with high O_3 concentrations, suggesting that biogenic emissions enhanced by higher temperatures can exceed the photochemical consumption of BVOCs. Based on the PMF analysis of non-methane VOCs measured by the Vocus-PTR-ToF-MS, six factors were resolved to represent the major sources and/or chemical transformation processes. During the entire measurement period, the TVOCs were largely composed of gaseous organic acid-related factors that formed from daytime photochemical oxidation of BVOCs. However, weakly-oxidized monoterpene products (e.g., $C_{10}H_{15}O_{1\text{-}3}^+$ and $C_{10}H_{17}O_{1\text{-}2}^+$) dominated the TVOCs during nighttime. These weakly-oxidized monoterpene products showed also higher concentrations in the particle phase during nighttime. In contrast, more-oxidized products of monoterpenes (e.g., $C_{10}H_{17}O_{4\text{-}5}^+$ and $C_{10}H_{15}O_{4\text{-}5}^+$) and isoprene oxidation products (e.g., $C_5H_9O_{1\text{-}4}^+$) in both gas and particle phases showed similar diurnal patterns with higher concentrations during daytime. This suggests that higher temperatures and intensive sunlight not only enhanced the biogenic emissions, but also promoted the photochemical oxidation of BVOCs. Combining the gas and particle data measured by the CHARON-PTR-ToF-MS and the Vocus-PTR-ToF-MS, we found that increasing RH can increase the particulate fraction of weakly-oxidized monoterpene products, which is consistent with the findings from recent simulation chamber studies (Surdu et al., 2023; Luo et al., 2024). Overall, this study demonstrates that multiple factors including meteorology, local anthropogenic emissions (e.g., from a BPP), and chemical transformation processes

https://doi.org/10.5194/egusphere-2024-1768
Preprint. Discussion started: 1 July 2024

influence the variations of BVOCs and their oxidation products in a typical stressed European forest. In addition, soil moisture played a minor role in the variations of BVOC concentrations in the limited observation period of this study. In the future, long-term field measurements are necessary to assess the impacts of droughts or bark beetle outbreaks on BVOC emissions.

Data availability

Data shown in the paper are available via the KIT data repository KITopen (link will be added).

Author contributions

JS, HS and RT conducted the field measurements. JS and GG carried out the data analysis of CHARON-PTR-ToF-MS and Vocus-PTR-ToF-MS respectively. NB and TL gave general comments for this paper. JS drafted the manuscript with contributions from all co-authors.

Competing interest

At least one of the (co-)authors is a member of the editorial board of Atmospheric Chemistry and Physics.

Acknowledgement

This work was supported by the Modular Observation Solutions for Earth Systems (MOSES) project, a novel observing system of the Helmholtz Association. Financial support by China Scholarship Council (CSC) for JS is gratefully acknowledged. The authors acknowledged Heye Bogena for providing daily soil moisture data as well as Christian Wesolek, Sergej Wedel, and Doreen Niether for their technical support in field measurement deployment.

https://doi.org/10.5194/egusphere-2024-1768
Preprint. Discussion started: 1 July 2024

References

Amin, H., Atkins, P. T., Russo, R. S., Brown, A. W., Sive, B., Hallar, A. G., and Huff Hartz, K. E.: Effect of Bark Beetle Infestation on Secondary Organic Aerosol Precursor Emissions, Environ. Sci. Technol., 46, 5696-5703, 10.1021/es204205m, 2012.

Atkinson, R.: Atmospheric chemistry of VOCs and NOx, Atmos. Environ., 34, 2063-2101, https://doi.org/10.1016/S1352-2310(99)00460-4, 2000.

Bakkaloglu, S., Lowry, D., Fisher, R. E., France, J. L., Brunner, D., Chen, H., and Nisbet, E. G.: Quantification of methane emissions from UK biogas plants, Waste Manage, 124, 82-93, https://doi.org/10.1016/j.wasman.2021.01.011, 2021.

Bogena, H. R., Huisman, J. A., Güntner, A., Hübner, C., Kusche, J., Jonard, F., Vey, S., and Vereecken, H.: Emerging methods for noninvasive sensing of soil moisture dynamics from field to catchment scale: a review, WIREs Water, 2, 635-647, https://doi.org/10.1002/wat2.1097, 2015.

Eichler, P., Muller, M., D'Anna, B., and Wisthaler, A.: A novel inlet system for online chemical analysis of semi-volatile submicron particulate matter, Atmos. Meas. Tech., 8, 1353-1360, 10.5194/amt-8-1353-2015, 2015.

Faiola, C. and Taipale, D.: Impact of insect herbivory on plant stress volatile emissions from trees: A synthesis of quantitative measurements and recommendations for future research, Atmospheric Environment: X, 5, 100060, https://doi.org/10.1016/j.aeaoa.2019.100060, 2020.

Ghimire, R. P., Kivimäenpää, M., Blomqvist, M., Holopainen, T., Lyytikäinen-Saarenmaa, P., and Holopainen, J. K.: Effect of bark beetle (Ips typographus L.) attack on bark VOC emissions of Norway spruce (Picea abies Karst.) trees, Atmospheric Environment, 126, 145-152, https://doi.org/10.1016/j.atmosenv.2015.11.049, 2016.

Gkatzelis, G. I., Coggon, M. M., McDonald, B. C., Peischl, J., Gilman, J. B., Aikin, K. C., Robinson, M. A., Canonaco, F., Prevot, A. S. H., Trainer, M., and Warneke, C.: Observations Confirm that Volatile Chemical Products Are a Major Source of Petrochemical Emissions in U.S. Cities, Environ. Sci. Technol., 55, 4332-4343, 10.1021/acs.est.0c05471, 2021.

Gkatzelis, G. I., Tillmann, R., Hohaus, T., Müller, M., Eichler, P., Xu, K. M., Schlag, P., Schmitt, S. H., Wegener, R., Kaminski, M., Holzinger, R., Wisthaler, A., and Kiendler-Scharr, A.: Comparison of three aerosol chemical characterization techniques utilizing PTR-ToF-MS: a study on freshly formed and aged biogenic SOA, Atmos. Meas. Tech., 11, 1481-1500, 10.5194/amt-11-1481-2018, 2018.

Guenther, A. B., Jiang, X., Heald, C. L., Sakulyanontvittaya, T., Duhl, T., Emmons, L. K., and Wang, X.: The Model of Emissions of Gases and Aerosols from Nature version 2.1 (MEGAN2.1): an extended and updated framework for modeling biogenic emissions, Geosci. Model Dev., 5, 1471-1492, 10.5194/gmd-5-1471-2012, 2012.

Hakola, H., Hellén, H., Hemmilä, M., Rinne, J., and Kulmala, M.: In situ measurements of volatile organic compounds in a boreal forest, Atmos. Chem. Phys., 12, 11665-11678, 10.5194/acp-12-11665-2012, 2012.

Hallquist, M., Wenger, J. C., Baltensperger, U., Rudich, Y., Simpson, D., Claeys, M., Dommen, J., Donahue, N. M., George, C., Goldstein, A. H., Hamilton, J. F., Herrmann, H., Hoffmann, T., Iinuma, Y., Jang, M., Jenkin, M. E., Jimenez, J. L., Kiendler-Scharr, A., Maenhaut, W., McFiggans, G., Mentel, T. F., Monod, A., Prévôt, A. S. H., Seinfeld, J. H., Surratt, J. D., Szmigielski, R., and Wildt, J.: The formation, properties and impact of secondary organic aerosol: current and emerging issues, Atmos. Chem. Phys., 9, 5155-5236, 10.5194/acp-9-5155-2009, 2009.

Hamilton, J. F., Webb, P. J., Lewis, A. C., and Reviejo, M. M.: Quantifying small molecules in secondary organic aerosol formed during the photo-oxidation of toluene with hydroxyl radicals, Atmospheric Environment, 39, 7263-7275, https://doi.org/10.1016/j.atmosenv.2005.09.006, 2005.

Hellén, H., Praplan, A. P., Tykkä, T., Ylivinkka, I., Vakkari, V., Bäck, J., Petäjä, T., Kulmala, M., and Hakola, H.: Long-term measurements of volatile organic compounds highlight the importance of sesquiterpenes for the atmospheric chemistry of a boreal forest, Atmos. Chem. Phys., 18, 13839-13863, 10.5194/acp-18-13839-2018, 2018.

Hersbach, H., Bell, B., Berrisford, P., Hirahara, S., Horányi, A., Muñoz-Sabater, J., Nicolas, J., Peubey, C., Radu, R., Schepers, D., Simmons, A., Soci, C., Abdalla, S., Abellan, X., Balsamo, G., Bechtold, P., Biavati, G., Bidlot, J., Bonavita, M., De Chiara, G., Dahlgren, P., Dee, D., Diamantakis, M., Dragani, R., Flemming, J., Forbes, R., Fuentes, M., Geer, A., Haimberger, L., Healy, S., Hogan, R.

https://doi.org/10.5194/egusphere-2024-1768
Preprint. Discussion started: 1 July 2024

J., Hólm, E., Janisková, M., Keeley, S., Laloyaux, P., Lopez, P., Lupu, C., Radnoti, G., de Rosnay, P., Rozum, I., Vamborg, F., Villaume, S., and Thépaut, J.-N.: The ERA5 global reanalysis, Quarterly Journal of the Royal Meteorological Society, 146, 1999-2049, https://doi.org/10.1002/qj.3803, 2020.

Huang, W., Saathoff, H., Shen, X., Ramisetty, R., Leisner, T., and Mohr, C.: Chemical Characterization of Highly Functionalized Organonitrates Contributing to Night-Time Organic Aerosol Mass Loadings and Particle Growth, Environ. Sci. Technol., 53, 1165-1174, 10.1021/acs.est.8b05826, 2019.

Huang, W., Li, H., Sarnela, N., Heikkinen, L., Tham, Y. J., Mikkilä, J., Thomas, S. J., Donahue, N. M., Kulmala, M., and Bianchi, F.: Measurement report: Molecular composition and volatility of gaseous organic compounds in a boreal forest – from volatile organic compounds to highly oxygenated organic molecules, Atmos. Chem. Phys., 21, 8961-8977, 10.5194/acp-21-8961-2021, 2021.

Isaacman-VanWertz, G., Yee, L. D., Kreisberg, N. M., Wernis, R., Moss, J. A., Hering, S. V., de Sá, S. S., Martin, S. T., Alexander, M. L., Palm, B. B., Hu, W., Campuzano-Jost, P., Day, D. A., Jimenez, J. L., Riva, M., Surratt, J. D., Viegas, J., Manzi, A., Edgerton, E., Baumann, K., Souza, R., Artaxo, P., and Goldstein, A. H.: Ambient Gas-Particle Partitioning of Tracers for Biogenic Oxidation, Environ. Sci. Tech., 50, 9952-9962, 10.1021/acs.est.6b01674, 2016.

Jaakkola, E., Gärtner, A., Jönsson, A. M., Ljung, K., Olsson, P. O., and Holst, T.: Spruce bark beetles (Ips typographus) cause up to 700 times higher bark BVOC emission rates compared to healthy Norway spruce (Picea abies), Biogeosciences, 20, 803-826, 10.5194/bg-20-803-2023, 2023.

Joó, É., Van Langenhove, H., Šimpraga, M., Steppe, K., Amelynck, C., Schoon, N., Müller, J. F., and Dewulf, J.: Variation in biogenic volatile organic compound emission pattern of Fagus sylvatica L. due to aphid infection, Atmospheric Environment, 44, 227-234, https://doi.org/10.1016/j.atmosenv.2009.10.007, 2010.

Jordan, A., Haidacher, S., Hanel, G., Hartungen, E., Mark, L., Seehauser, H., Schottkowsky, R., Sulzer, P., and Mark, T. D.: A high resolution and high sensitivity proton-transfer-reaction time-of-flight mass spectrometer (PTR-TOF-MS), International Journal of Mass Spectrometry, 286, 122-128, 10.1016/j.ijms.2009.07.005, 2009.

Kari, E., Miettinen, P., Yli-Pirilä, P., Virtanen, A., and Faiola, C. L.: PTR-ToF-MS product ion distributions and humidity-dependence of biogenic volatile organic compounds, International Journal of Mass Spectrometry, 430, 87-97, https://doi.org/10.1016/j.ijms.2018.05.003, 2018.

Kari, E., Faiola, C., Isokääntä, S., Miettinen, P., Yli-Pirilä, P., Buchholz, A., Kivimäenpää, M., Mikkonen, S., Holopainen, J., and Virtanen, A.: Time-resolved characterization of biotic stress emissions from Scots pines being fed upon by pine weevil by means of PTR-ToF-MS, Boreal Environment Research, 24, 1-1–11, 2019.

Kim, S., Karl, T., Helmig, D., Daly, R., Rasmussen, R., and Guenther, A.: Measurement of atmospheric sesquiterpenes by proton transfer reaction-mass spectrometry (PTR-MS), Atmos. Meas. Tech., 2, 99-112, 10.5194/amt-2-99-2009, 2009.

Kleist, E., Mentel, T. F., Andres, S., Bohne, A., Folkers, A., Kiendler-Scharr, A., Rudich, Y., Springer, M., Tillmann, R., and Wildt, J.: Irreversible impacts of heat on the emissions of monoterpenes, sesquiterpenes, phenolic BVOC and green leaf volatiles from several tree species, Biogeosciences, 9, 5111-5123, 10.5194/bg-9-5111-2012, 2012.

Krechmer, J., Lopez-Hilfiker, F., Koss, A., Hutterli, M., Stoermer, C., Deming, B., Kimmel, J., Warneke, C., Holzinger, R., Jayne, J., Worsnop, D., Fuhrer, K., Gonin, M., and de Gouw, J.: Evaluation of a New Reagent-Ion Source and Focusing Ion–Molecule Reactor for Use in Proton-Transfer-Reaction Mass Spectrometry, Analytical Chemistry, 90, 12011-12018, 10.1021/acs.analchem.8b02641, 2018.

Lannuque, V., D'Anna, B., Kostenidou, E., Couvidat, F., Martinez-Valiente, A., Eichler, P., Wisthaler, A., Müller, M., Temime-Roussel, B., Valorso, R., and Sartelet, K.: Gas–particle partitioning of toluene oxidation products: an experimental and modeling study, Atmos. Chem. Phys., 23, 15537-15560, 10.5194/acp-23-15537-2023, 2023.

Lee, B. H., Lopez-Hilfiker, F. D., D'Ambro, E. L., Zhou, P., Boy, M., Petäjä, T., Hao, L., Virtanen, A., and Thornton, J. A.: Semi-volatile and highly oxygenated gaseous and particulate organic compounds observed above a boreal forest canopy, Atmos. Chem. Phys., 18, 11547-11562, 10.5194/acp-18-11547-2018, 2018.

https://doi.org/10.5194/egusphere-2024-1768
Preprint. Discussion started: 1 July 2024

Leglise, J., Müller, M., Piel, F., Otto, T., and Wisthaler, A.: Bulk Organic Aerosol Analysis by Proton-Transfer-Reaction Mass Spectrometry: An Improved Methodology for the Determination of Total Organic Mass, O:C and H:C Elemental Ratios, and the Average Molecular Formula, Anal. Chem., 91, 12619-12624, 10.1021/acs.analchem.9b02949, 2019.

Li, H., Riva, M., Rantala, P., Heikkinen, L., Daellenbach, K., Krechmer, J. E., Flaud, P. M., Worsnop, D., Kulmala, M., Villenave, E., Perraudin, E., Ehn, M., and Bianchi, F.: Terpenes and their oxidation products in the French Landes forest: insights from Vocus PTR-TOF measurements, Atmos. Chem. Phys., 20, 1941-1959, 10.5194/acp-20-1941-2020, 2020.

Li, H., Canagaratna, M. R., Riva, M., Rantala, P., Zhang, Y., Thomas, S., Heikkinen, L., Flaud, P. M., Villenave, E., Perraudin, E., Worsnop, D., Kulmala, M., Ehn, M., and Bianchi, F.: Atmospheric organic vapors in two European pine forests measured by a Vocus PTR-TOF: insights into monoterpene and sesquiterpene oxidation processes, Atmos. Chem. Phys., 21, 4123-4147, 10.5194/acp-21-4123-2021, 2021a.

Li, X. B., Yuan, B., Wang, S., Wang, C., Lan, J., Liu, Z., Song, Y., He, X., Huangfu, Y., Pei, C., Cheng, P., Yang, S., Qi, J., Wu, C., Huang, S., You, Y., Chang, M., Zheng, H., Yang, W., Wang, X., and Shao, M.: Variations and sources of volatile organic compounds (VOCs) in urban region: insights from measurements on a tall tower, Atmos. Chem. Phys., 22, 10567-10587, 10.5194/acp-22-10567-2022, 2022.

Li, Y., Zhao, J., Wang, Y., Seinfeld, J. H., and Zhang, R.: Multigeneration Production of Secondary Organic Aerosol from Toluene Photooxidation, Environ. Sci. Technol., 55, 8592-8603, 10.1021/acs.est.1c02026, 2021b.

Loreto, F. and Schnitzler, J.-P.: Abiotic stresses and induced BVOCs, Trends in Plant Science, 15, 154-166, 10.1016/j.tplants.2009.12.006, 2010.

Luo, H., Guo, Y., Shen, H., Huang, D. D., Zhang, Y., and Zhao, D.: Effect of relative humidity on the molecular composition of secondary organic aerosols from α-pinene ozonolysis, Environmental Science: Atmospheres, 10.1039/D3EA00149K, 2024.

Mermet, K., Perraudin, E., Dusanter, S., Sauvage, S., Léonardis, T., Flaud, P.-M., Bsaibes, S., Kammer, J., Michoud, V., Gratien, A., Cirtog, M., Al Ajami, M., Truong, F., Batut, S., Hecquet, C., Doussin, J.-F., Schoemaecker, C., Gros, V., Locoge, N., and Villenave, E.: Atmospheric reactivity of biogenic volatile organic compounds in a maritime pine forest during the LANDEX episode 1 field campaign, Sci. Total Environ., 756, 144129, https://doi.org/10.1016/j.scitotenv.2020.144129, 2021.

Mohr, C., Lopez-Hilfiker, F. D., Yli-Juuti, T., Heitto, A., Lutz, A., Hallquist, M., D'Ambro, E. L., Rissanen, M. P., Hao, L., Schobesberger, S., Kulmala, M., Mauldin III, R. L., Makkonen, U., Sipilä, M., Petäjä, T., and Thornton, J. A.: Ambient observations of dimers from terpene oxidation in the gas phase: Implications for new particle formation and growth, Geophys. Res. Lett., 44, 2958-2966, https://doi.org/10.1002/2017GL072718, 2017.

Montzka, C., Bayat, B., Tewes, A., Mengen, D., and Vereecken, H.: Spruce Crown Transparency Levels Detected from Sentinel-2 Using Google Earth Engine, 2021 IEEE International Geoscience and Remote Sensing Symposium IGARSS, 11-16 July 2021, 5815-5817, 10.1109/IGARSS47720.2021.9553506,

Muller, M., Eicher, P., D'Anna, B., Tan, W., and Wisthaler, A.: Direct Sampling and Analysis of Atmospheric Particulate Organic Matter by Proton-Transfer-Reaction Mass Spectrometry, Analytical Chemistry, 89, 10889-10897, 10.1021/acs.analchem.7b02582, 2017.

Müller, M., Eichler, P., D'Anna, B., Tan, W., and Wisthaler, A.: Direct Sampling and Analysis of Atmospheric Particulate Organic Matter by Proton-Transfer-Reaction Mass Spectrometry, Analytical Chemistry, 89, 10889-10897, 10.1021/acs.analchem.7b02582, 2017.

Ng, N. L., Canagaratna, M. R., Jimenez, J. L., Chhabra, P. S., Seinfeld, J. H., and Worsnop, D. R.: Changes in organic aerosol composition with aging inferred from aerosol mass spectra, Atmos. Chem. Phys., 11, 6465-6474, 10.5194/acp-11-6465-2011, 2011.

Ng, N. L., Canagaratna, M. R., Zhang, Q., Jimenez, J. L., Tian, J., Ulbrich, I. M., Kroll, J. H., Docherty, K. S., Chhabra, P. S., Bahreini, R., Murphy, S. M., Seinfeld, J. H., Hildebrandt, L., Donahue, N. M., DeCarlo, P. F., Lanz, V. A., Prevot, A. S. H., Dinar, E., Rudich, Y., and Worsnop, D. R.: Organic aerosol components observed in Northern Hemispheric datasets from Aerosol Mass Spectrometry, Atmos. Chem. Phys., 10, 4625-4641, 10.5194/acp-10-4625-2010, 2010.

https://doi.org/10.5194/egusphere-2024-1768
Preprint. Discussion started: 1 July 2024

Paatero, P. and Tapper, U.: Positive matrix factorization: A non-negative factor model with optimal utilization of error estimates of data values, Environmetrics, 5, 111-126, https://doi.org/10.1002/env.3170050203, 1994.

Pagonis, D., Sekimoto, K., and de Gouw, J.: A Library of Proton-Transfer Reactions of H3O+ Ions Used for Trace Gas Detection, Journal of the American Society for Mass Spectrometry, 30, 1330-1335, 10.1007/s13361-019-02209-3, 2019.

Papurello, D., Soukoulis, C., Schuhfried, E., Cappellin, L., Gasperi, F., Silvestri, S., Santarelli, M., and Biasioli, F.: Monitoring of volatile compound emissions during dry anaerobic digestion of the Organic Fraction of Municipal Solid Waste by Proton Transfer Reaction Time-of-Flight Mass Spectrometry, Bioresource Technology, 126, 254-265, https://doi.org/10.1016/j.biortech.2012.09.033, 2012.

Peng, Y., Wang, H., Gao, Y., Jing, S., Zhu, S., Huang, D., Hao, P., Lou, S., Cheng, T., Huang, C., and Zhang, X.: Real-time measurement of phase partitioning of organic compounds using a proton-transfer-reaction time-of-flight mass spectrometer coupled to a CHARON inlet, Atmos. Meas. Tech., 16, 15-28, 10.5194/amt-16-15-2023, 2023.

Pernov, J. B., Bossi, R., Lebourgeois, T., Nøjgaard, J. K., Holzinger, R., Hjorth, J. L., and Skov, H.: Atmospheric VOC measurements at a High Arctic site: characteristics and source apportionment, Atmos. Chem. Phys., 21, 2895-2916, 10.5194/acp-21-2895-2021, 2021.

Piel, F., Müller, M., Winkler, K., Skytte af Sätra, J., and Wisthaler, A.: Introducing the extended volatility range proton-transfer-reaction mass spectrometer (EVR PTR-MS), Atmos. Meas. Tech., 14, 1355-1363, 10.5194/amt-14-1355-2021, 2021.

Salazar Gómez, J. I., Lohmann, H., and Krassowski, J.: Determination of volatile organic compounds from biowaste and co-fermentation biogas plants by single-sorbent adsorption, Chemosphere, 153, 48-57, https://doi.org/10.1016/j.chemosphere.2016.02.128, 2016.

Scheftelowitz, M., Becker, R., and Thrän, D.: Improved power provision from biomass: A retrospective on the impacts of German energy policy, Biomass and Bioenergy, 111, 1-12, https://doi.org/10.1016/j.biombioe.2018.01.010, 2018.

Shrivastava, M., Cappa, C. D., Fan, J., Goldstein, A. H., Guenther, A. B., Jimenez, J. L., Kuang, C., Laskin, A., Martin, S. T., Ng, N. L., Petaja, T., Pierce, J. R., Rasch, P. J., Roldin, P., Seinfeld, J. H., Shilling, J., Smith, J. N., Thornton, J. A., Volkamer, R., Wang, J., Worsnop, D. R., Zaveri, R. A., Zelenyuk, A., and Zhang, Q.: Recent advances in understanding secondary organic aerosol: Implications for global climate forcing, Reviews of Geophysics, 55, 509-559, https://doi.org/10.1002/2016RG000540, 2017.

Sindelarova, K., Granier, C., Bouarar, I., Guenther, A., Tilmes, S., Stavrakou, T., Müller, J. F., Kuhn, U., Stefani, P., and Knorr, W.: Global data set of biogenic VOC emissions calculated by the MEGAN model over the last 30 years, Atmos. Chem. Phys., 14, 9317-9341, 10.5194/acp-14-9317-2014, 2014.

Smiatek, G. and Steinbrecher, R.: Temporal and spatial variation of forest VOC emissions in Germany in the decade 1994–2003, Atmos. Environ., 40, 166-177, https://doi.org/10.1016/j.atmosenv.2005.11.071, 2006.

Song, J., Saathoff, H., Gao, L., Gebhardt, R., Jiang, F., Vallon, M., Bauer, J., Norra, S., and Leisner, T.: Variations of PM2.5 sources in the context of meteorology and seasonality at an urban street canyon in Southwest Germany, Atmos. Environ., 119147, https://doi.org/10.1016/j.atmosenv.2022.119147, 2022.

Surdu, M., Lamkaddam, H., Wang, D. S., Bell, D. M., Xiao, M., Lee, C. P., Li, D., Caudillo, L., Marie, G., Scholz, W., Wang, M., Lopez, B., Piedehierro, A. A., Ataei, F., Baalbaki, R., Bertozzi, B., Bogert, P., Brasseur, Z., Dada, L., Duplissy, J., Finkenzeller, H., He, X.-C., Höhler, K., Korhonen, K., Krechmer, J. E., Lehtipalo, K., Mahfouz, N. G. A., Manninen, H. E., Marten, R., Massabò, D., Mauldin, R., Petäjä, T., Pfeifer, J., Philippov, M., Rörup, B., Simon, M., Shen, J., Umo, N. S., Vogel, F., Weber, S. K., Zauner-Wieczorek, M., Volkamer, R., Saathoff, H., Möhler, O., Kirkby, J., Worsnop, D. R., Kulmala, M., Stratmann, F., Hansel, A., Curtius, J., Welti, A., Riva, M., Donahue, N. M., Baltensperger, U., and El Haddad, I.: Molecular Understanding of the Enhancement in Organic Aerosol Mass at High Relative Humidity, Environ. Sci. Technol., 57, 2297-2309, 10.1021/acs.est.2c04587, 2023.

https://doi.org/10.5194/egusphere-2024-1768
Preprint. Discussion started: 1 July 2024

Tani, A., Hayward, S., and Hewitt, C. N.: Measurement of monoterpenes and related compounds by proton transfer reaction-mass spectrometry (PTR-MS), International Journal of Mass Spectrometry, 223-224, 561-578, https://doi.org/10.1016/S1387-3806(02)00880-1, 2003.

Teskey, R., Wertin, T., Bauweraerts, I., Ameye, M., McGuire, M. A., and Steppe, K.: Responses of tree species to heat waves and extreme heat events, Plant, Cell & Environment, 38, 1699-1712, https://doi.org/10.1111/pce.12417, 2015.

Tillmann, R., Hallquist, M., Jonsson, Å. M., Kiendler-Scharr, A., Saathoff, H., Iinuma, Y., and Mentel, T. F.: Influence of relative humidity and temperature on the production of pinonaldehyde and OH radicals from the ozonolysis of α-pinene, Atmos. Chem. Phys., 10, 7057-7072, 10.5194/acp-10-7057-2010, 2010.

Vermeuel, M. P., Novak, G. A., Kilgour, D. B., Claflin, M. S., Lerner, B. M., Trowbridge, A. M., Thom, J., Cleary, P. A., Desai, A. R., and Bertram, T. H.: Observations of biogenic volatile organic compounds over a mixed temperate forest during the summer to autumn transition, Atmos. Chem. Phys., 23, 4123-4148, 10.5194/acp-23-4123-2023, 2023.

Vestenius, M., Hopke, P. K., Lehtipalo, K., Petäjä, T., Hakola, H., and Hellén, H.: Assessing volatile organic compound sources in a boreal forest using positive matrix factorization (PMF), Atmos. Environ., 259, 118503, https://doi.org/10.1016/j.atmosenv.2021.118503, 2021.

von Hessberg, C., von Hessberg, P., Pöschl, U., Bilde, M., Nielsen, O. J., and Moortgat, G. K.: Temperature and humidity dependence of secondary organic aerosol yield from the ozonolysis of β-pinene, Atmos. Chem. Phys., 9, 3583-3599, 10.5194/acp-9-3583-2009, 2009.

Wang, L., Slowik, J. G., Tripathi, N., Bhattu, D., Rai, P., Kumar, V., Vats, P., Satish, R., Baltensperger, U., Ganguly, D., Rastogi, N., Sahu, L. K., Tripathi, S. N., and Prévôt, A. S. H.: Source characterization of volatile organic compounds measured by proton-transfer-reaction time-of-flight mass spectrometers in Delhi, India, Atmos. Chem. Phys., 20, 9753-9770, 10.5194/acp-20-9753-2020, 2020.

Weber, U., Attinger, S., Baschek, B., Boike, J., Borchardt, D., Brix, H., Brüggemann, N., Bussmann, I., Dietrich, P., Fischer, P., Greinert, J., Hajnsek, I., Kamjunke, N., Kerschke, D., Kiendler-Scharr, A., Körtzinger, A., Kottmeier, C., Merz, B., Merz, R., Riese, M., Schloter, M., Schmid, H., Schnitzler, J.-P., Sachs, T., Schütze, C., Tillmann, R., Vereecken, H., Wieser, A., and Teutsch, G.: MOSES: A Novel Observation System to Monitor Dynamic Events across Earth Compartments, B Am Meteorol Soc, 103, E339-E348, 10.1175/bams-d-20-0158.1, 2022.

Wennberg, P. O., Bates, K. H., Crounse, J. D., Dodson, L. G., McVay, R. C., Mertens, L. A., Nguyen, T. B., Praske, E., Schwantes, R. H., Smarte, M. D., St Clair, J. M., Teng, A. P., Zhang, X., and Seinfeld, J. H.: Gas-Phase Reactions of Isoprene and Its Major Oxidation Products, Chem Rev, 118, 3337-3390, 10.1021/acs.chemrev.7b00439, 2018.

Wu, R., Pan, S., Li, Y., and Wang, L.: Atmospheric Oxidation Mechanism of Toluene, The Journal of Physical Chemistry A, 118, 4533-4547, 10.1021/jp500077f, 2014.

Yáñez-Serrano, A. M., Bach, A., Bartolomé-Català, D., Matthaios, V., Seco, R., Llusià, J., Filella, I., and Peñuelas, J.: Dynamics of volatile organic compounds in a western Mediterranean oak forest, Atmos. Environ., 257, 118447, https://doi.org/10.1016/j.atmosenv.2021.118447, 2021.

Yáñez-Serrano, A. M., Nölscher, A. C., Williams, J., Wolff, S., Alves, E., Martins, G. A., Bourtsoukidis, E., Brito, J., Jardine, K., Artaxo, P., and Kesselmeier, J.: Diel and seasonal changes of biogenic volatile organic compounds within and above an Amazonian rainforest, Atmos. Chem. Phys., 15, 3359-3378, 10.5194/acp-15-3359-2015, 2015.

Yáñez-Serrano, A. M., Bourtsoukidis, E., Alves, E. G., Bauwens, M., Stavrakou, T., Llusià, J., Filella, I., Guenther, A., Williams, J., Artaxo, P., Sindelarova, K., Doubalova, J., Kesselmeier, J., and Peñuelas, J.: Amazonian biogenic volatile organic compounds under global change, Global Change Biology, 26, 4722-4751, https://doi.org/10.1111/gcb.15185, 2020.

Yatavelli, R. L. N., Stark, H., Thompson, S. L., Kimmel, J. R., Cubison, M. J., Day, D. A., Campuzano-Jost, P., Palm, B. B., Hodzic, A., Thornton, J. A., Jayne, J. T., Worsnop, D. R., and Jimenez, J. L.: Semicontinuous measurements of gas–particle partitioning of organic acids in a ponderosa pine forest using a MOVI-HRToF-CIMS, Atmos. Chem. Phys., 14, 1527-1546, 10.5194/acp-14-1527-2014, 2014.

Yuan, B., Shao, M., de Gouw, J., Parrish, D. D., Lu, S., Wang, M., Zeng, L., Zhang, Q., Song, Y., Zhang, J., and Hu, M.: Volatile organic compounds (VOCs) in urban air: How chemistry affects the

https://doi.org/10.5194/egusphere-2024-1768
Preprint. Discussion started: 1 July 2024

interpretation of positive matrix factorization (PMF) analysis, Journal of Geophysical Research: Atmospheres, 117, https://doi.org/10.1029/2012JD018236, 2012.

Zaytsev, A., Koss, A. R., Breitenlechner, M., Krechmer, J. E., Nihill, K. J., Lim, C. Y., Rowe, J. C., Cox, J. L., Moss, J., Roscioli, J. R., Canagaratna, M. R., Worsnop, D. R., Kroll, J. H., and Keutsch, F. N.: Mechanistic study of the formation of ring-retaining and ring-opening products from the oxidation of aromatic compounds under urban atmospheric conditions, Atmos. Chem. Phys., 19, 15117-15129, 10.5194/acp-19-15117-2019, 2019.

Zhang, X., McVay, R. C., Huang, D. D., Dalleska, N. F., Aumont, B., Flagan, R. C., and Seinfeld, J. H.: Formation and evolution of molecular products in α-pinene secondary organic aerosol, Proceedings of the National Academy of Sciences, 112, 14168-14173, doi:10.1073/pnas.1517742112, 2015.

https://doi.org/10.5194/egusphere-2024-1768
Preprint. Discussion started: 1 July 2024

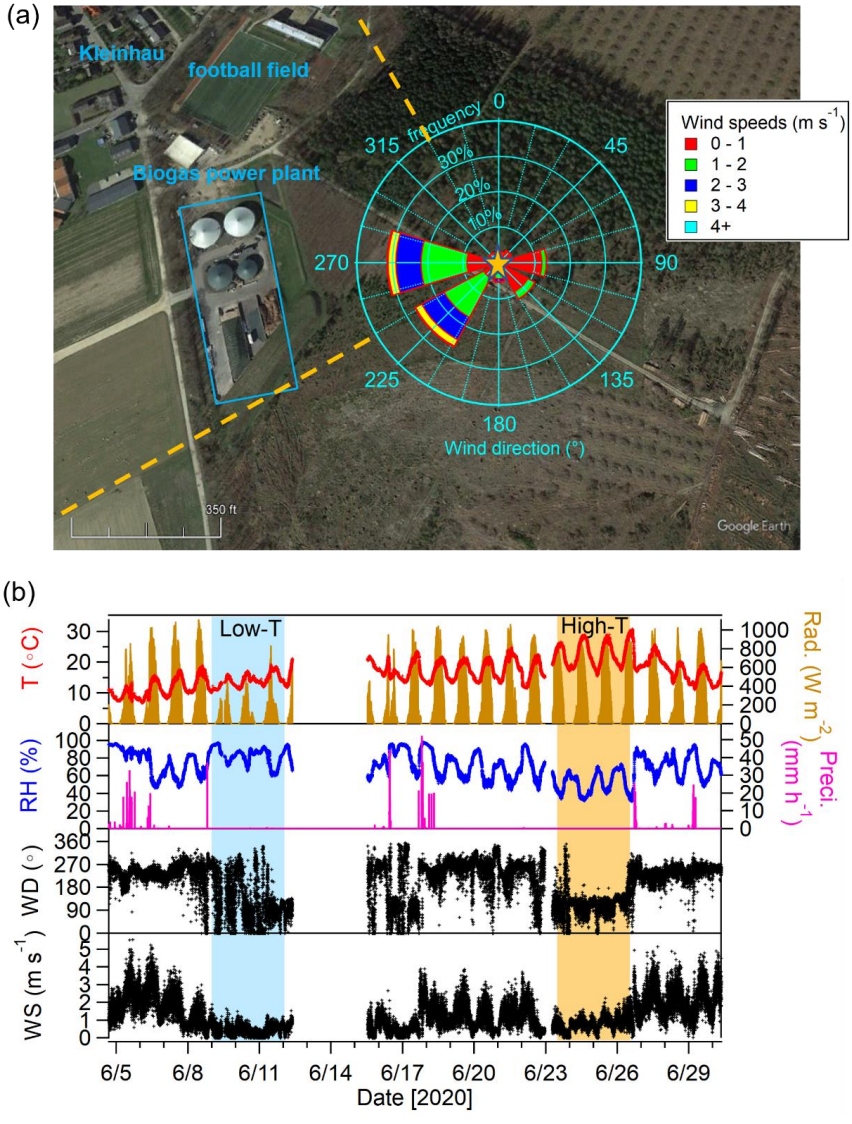

Figure 1. (a) Location of the sampling site (orange star) with the centered wind rose for the entire measurement period (©Google Earth). Two orange dash lines are shown for distinguishing the wind sectors. Data within the wind sector of 240-330 ° are considered to be influenced by the biogas power plant (blue rectangle) and/or residential areas of Kleinhau, while the wind sector of 0-240 ° is influenced by the forest; (b) time series of meteorological parameters including ambient temperature (T), relative humidity (RH), wind direction and speed (WD and WS), radiation and precipitation. The blue and orange shaded areas mark the low-T and high-T episodes.

https://doi.org/10.5194/egusphere-2024-1768
Preprint. Discussion started: 1 July 2024

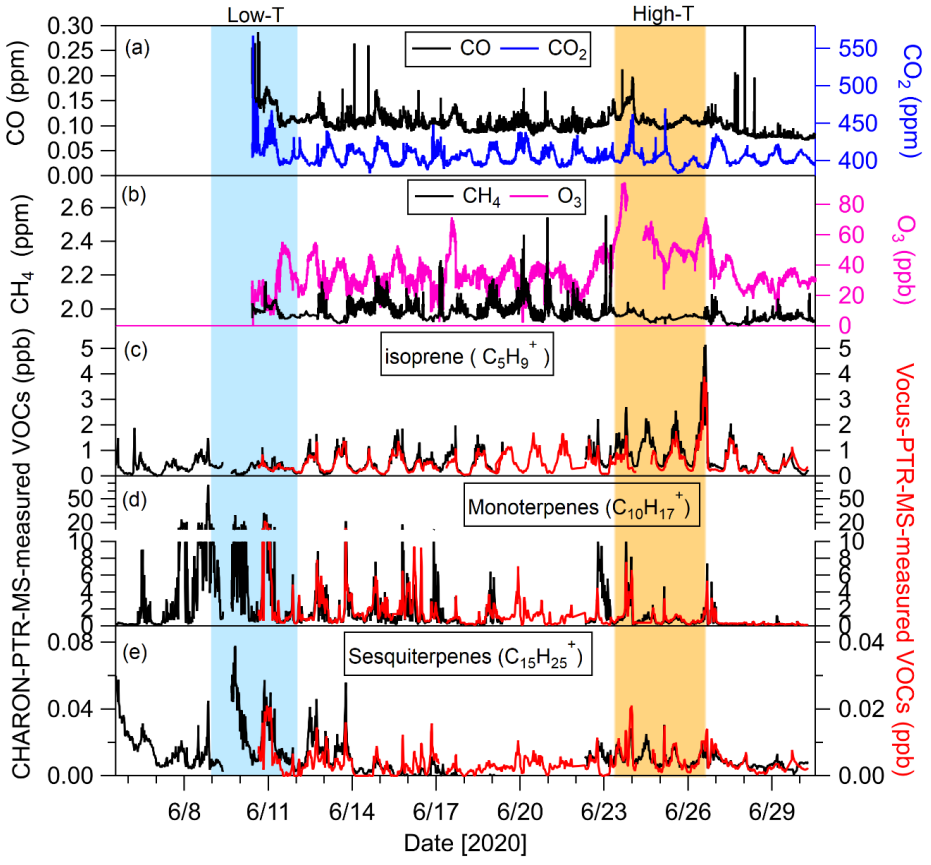

964

965 **Figure 2.** Time series of gas concentrations: (a) CO and CO_2; (b) CH_4 and O_3; (c-e) isoprene,
966 monoterpenes, sesquiterpenes measured by the CHARON-PTR-MS (black lines) and Vocus-
967 PTR-MS (red lines) respectively. The blue and yellow shaded areas mark the low-T and high-
968 T episodes.

https://doi.org/10.5194/egusphere-2024-1768
Preprint. Discussion started: 1 July 2024

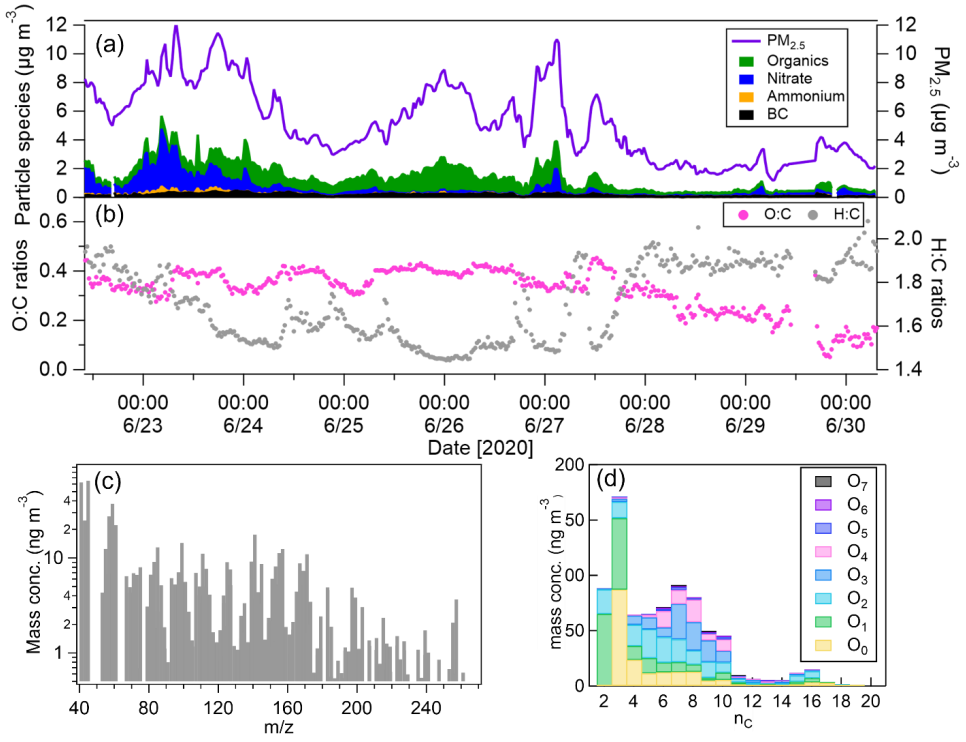

969

970 **Figure 3.** Time series of (a) mass concentrations of $PM_{2.5}$, BC and semi-volatile particle species
971 (organics, nitrate and ammonium) measured by the CHARON-PTR-ToF-MS simultaneously
972 available during 22nd-30th June; (b) oxygen to carbon (O:C) and hydrogen to carbon (H:C) ratios
973 of organics. (c) average mass spectrum of organics; (d) mass distributions of organics associated
974 with $C_xH_yO_{0\text{-}7}^+$ resolved by the carbon and oxygen numbers (n_C and n_O).

https://doi.org/10.5194/egusphere-2024-1768
Preprint. Discussion started: 1 July 2024

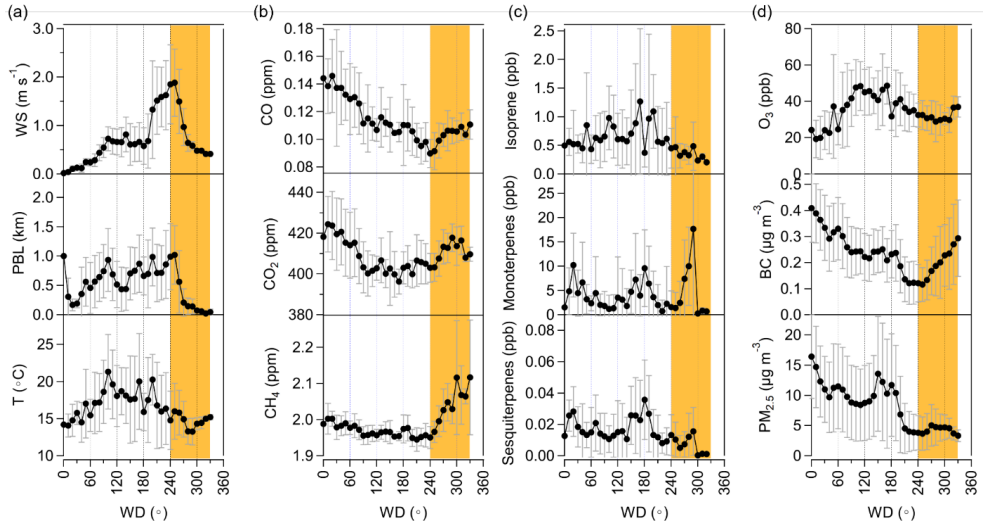

Figure 4. Variations of (a) wind speed (WS), planetary boundary layer (PBL) and ambient temperature; (b) concentrations of CO, CO_2 and CH_4; (c) concentrations of isoprene, monoterpenes and sesquiterpenes; and (d) concentrations of O_3, BC and $PM_{2.5}$ mass as a function of wind direction (WD). The black dots and whiskers represent the mean values and standard deviations in each WD bin of 10 º. The orange shaded areas mark the WD sector of the biogas power plant and/or residential areas (240-330 º).

https://doi.org/10.5194/egusphere-2024-1768
Preprint. Discussion started: 1 July 2024

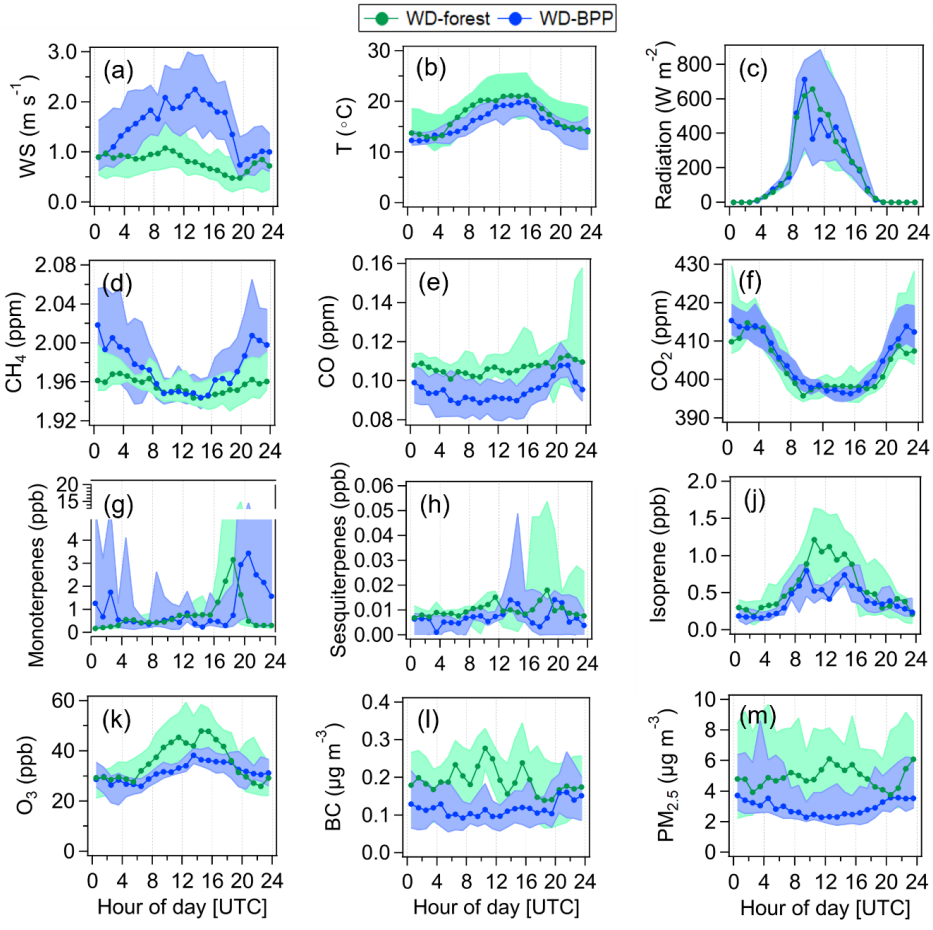

Figure 5. Diurnal variations of (a-c) wind speeds, ambient temperature and global radiation; (d-f) CH_4, CO and CO_2; (g-j) monoterpenes, sesquiterpenes and isoprene; (k-m) O_3, BC, $PM_{2.5}$. The green and blue markers represent the median values calculated for the measurement periods when the winds coming from the forest (WD-forest) and the biogas power plant (WD-BPP), respectively. The shaded areas represent the 25^{th} and 75^{th} percentiles.

https://doi.org/10.5194/egusphere-2024-1768
Preprint. Discussion started: 1 July 2024

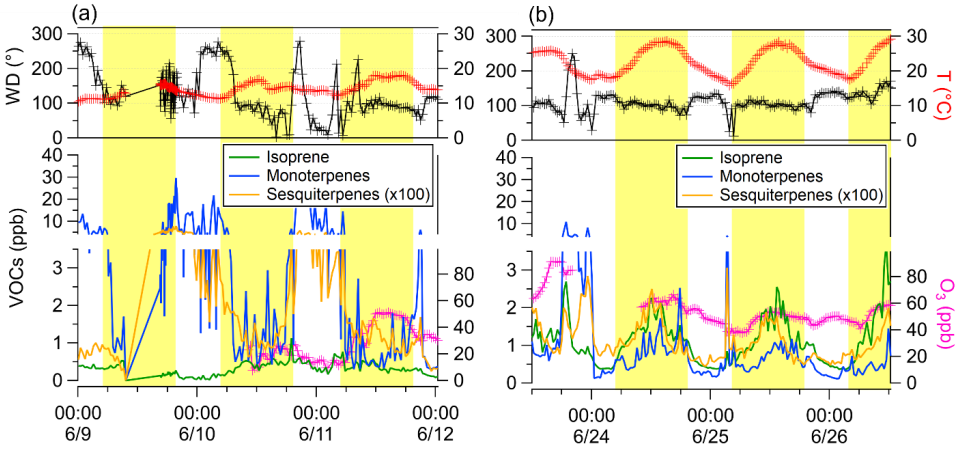

Figure 6. Time series of wind direction, ambient temperature, isoprene, monoterpenes, sesquiterpenes and O_3 during the low-T (a) and high-T (b) episodes. The yellow shaded areas mark the daytime from 4:00-20:00 UTC.

https://doi.org/10.5194/egusphere-2024-1768
Preprint. Discussion started: 1 July 2024

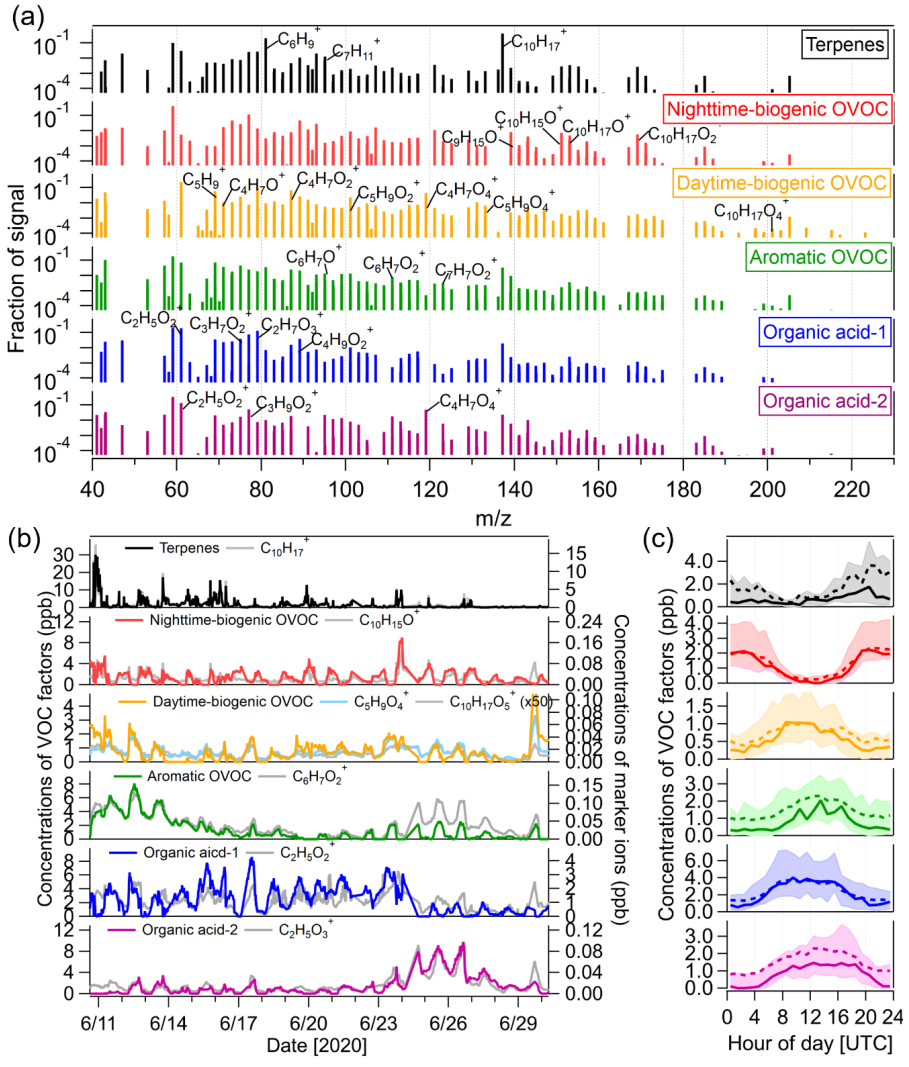

Figure 7. (a) Factor profiles of six VOC factors resolved from the PMF analysis of Vocus-PTR-ToF-MS data; (b) time series of six VOC factors with each correlated fingerprint VOC ions; (c) diurnal variations of VOC factors during the entire measurement campaign. The solid and dash lines represent median and mean values respectively and the shaded areas represent the 25th and 75th percentiles.

https://doi.org/10.5194/egusphere-2024-1768
Preprint. Discussion started: 1 July 2024

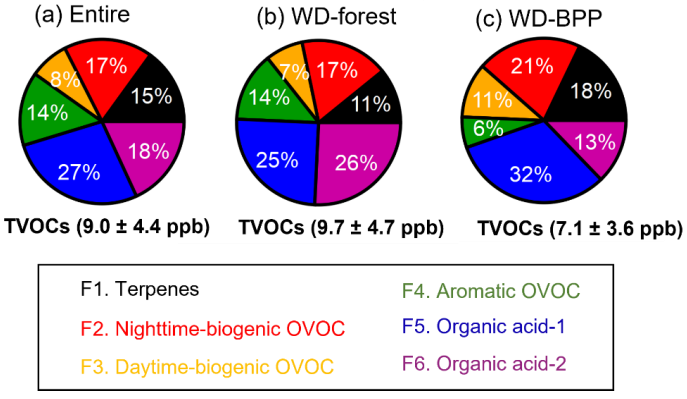

Figure 8. Average contribution of the VOC factors (terpenes, nighttime-biogenic OVOC, daytime-biogenic OVOC, aromatic OVOC, organic acid-1 and organic acid-2) to total VOCs (TVOCs) measured by the Vocus-PTR-ToF-MS for the entire measurement campaign and the WD-forest and WD-BPP groups.

https://doi.org/10.5194/egusphere-2024-1768
Preprint. Discussion started: 1 July 2024

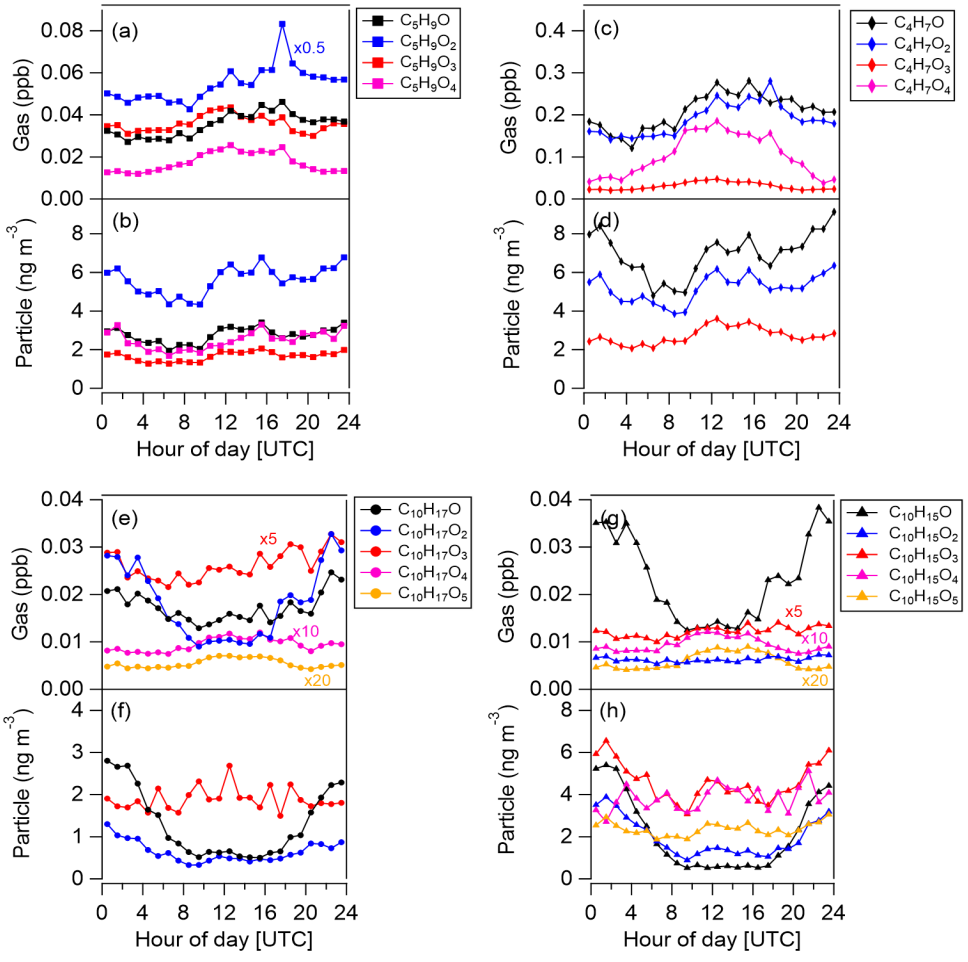

Figure 9. Diurnal variations of (a-d) concentrations of isoprene oxidation products ($C_5H_9O_{1\text{-}4}^+$ and $C_4H_7O_{1\text{-}4}^+$) in gas and particle phases; (e-h) concentrations of monoterpene oxidation products ($C_{10}H_{17}O_{1\text{-}5}^+$ and $C_{10}H_{15}O_{1\text{-}5}^+$) in gas and particle phases calculated for the measurement period of 22nd-30th of June. Gas- and particle-phase data were taken from the Vocus-PTR-ToF-MS and CHARON-PTR-ToF-MS measurements, respectively. The higher-oxidized particle-phase products from isoprene ($C_4H_7O_4^+$) and monoterpenes ($C_{10}H_{17}O_{4\text{-}5}^+$) cannot be detected by the CHARON-PTR-ToF-MS.

https://doi.org/10.5194/egusphere-2024-1768
Preprint. Discussion started: 1 July 2024

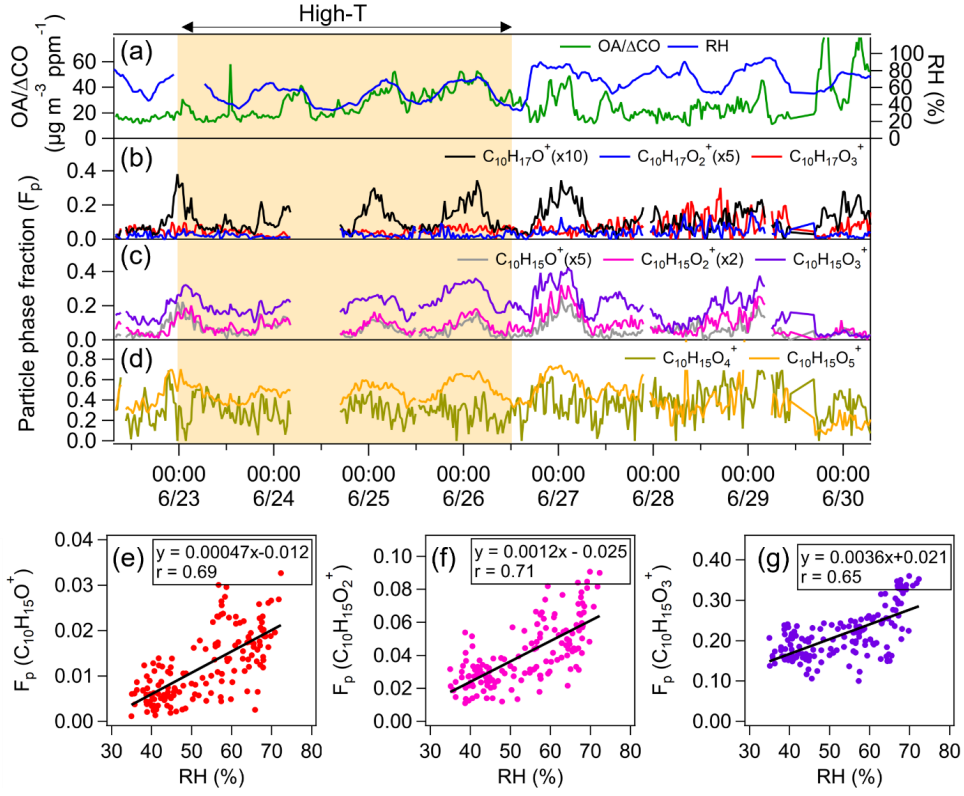

Figure 10. Time series of (a) OA/ΔCO and relative humidity (RH); (b-d) particle phase fraction of monoterpene oxidation products ($C_{10}H_{17}O_{1\text{-}3}^{+}$ and $C_{10}H_{15}O_{1\text{-}5}^{+}$) from 22nd-30th of June. The yellow shaded area marks the high-T episode. (e-f) Correlations of the time series of particle phase fraction of $C_{10}H_{15}O_{1\text{-}3}^{+}$ with RH during high-T episode.